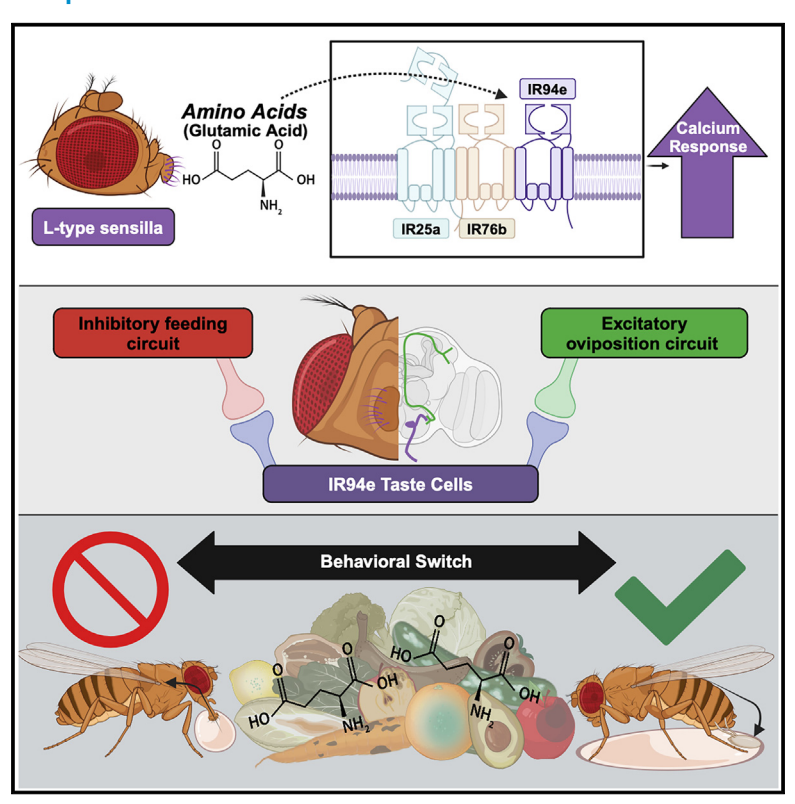
Taste cells expressing *lonotropic Receptor 94e* reciprocally impact feeding and egg laying in *Drosophila*

Graphical abstract



Authors

Jacqueline Guillemin, Jinfang Li, Viktoriya Li, ..., Liam Kelliher, Michael D. Gordon, Molly Stanley

Correspondence

michael.gordon@ubc.ca (M.D.G.), molly.stanley@uvm.edu (M.S.)

In brief

Guillemin et al. describe how a distinct set of taste cells on the labellum that express *IR94e* function in behavior. They find that IR94e chemosensory neurons discourage feeding but increase egg laying and reveal that amino acids, particularly glutamate, stimulate IR94e cells through the IR94e receptor.

Highlights

- Activation of IR94e taste cells on the labellum produces mild feeding aversion
- Neural circuits connect IR94e neurons to OviDNs, and IR94e activity increases egg laying
- IR94e taste cells respond to certain amino acids through an IR94e receptor complex
- IR94e mutants have changes in feeding and oviposition behaviors to amino acids







Article

Taste cells expressing *lonotropic Receptor 94e* reciprocally impact feeding and egg laying in *Drosophila*

Jacqueline Guillemin, Jinfang Li, Viktoriya Li, Sasha A.T. McDowell, Kayla Audette, Grace Davis, Meghan Jelen, Samy Slamani, Liam Kelliher, Michael D. Gordon, 4 and Molly Stanley 1, 3, *

SUMMARY

Chemosensory cells across the body of *Drosophila melanogaster* evaluate the environment to prioritize certain behaviors. Previous mapping of gustatory receptor neurons (GRNs) on the fly labellum identified a set of neurons in L-type sensilla that express *Ionotropic Receptor 94e* (IR94e), but the impact of IR94e GRNs on behavior remains unclear. We used optogenetics and chemogenetics to activate IR94e neurons and found that they drive mild feeding suppression but enhance egg laying. *In vivo* calcium imaging revealed that IR94e GRNs respond strongly to certain amino acids, including glutamate, and that IR94e plus co-receptors IR25a and IR76b are required for amino acid detection. Furthermore, *IR94e* mutants show behavioral changes to solutions containing amino acids, including increased consumption and decreased egg laying. Overall, our results suggest that IR94e GRNs on the fly labellum discourage feeding and encourage egg laying as part of an important behavioral switch in response to certain chemical cues.

INTRODUCTION

Animal chemosensation is essential for assessing environmental cues to drive advantageous behaviors. In a variety of flying insects, behaviors such as feeding, mating, and oviposition are preceded by contact between chemical cues and receptors that are present in the mouthparts, legs, wings, and ovipositor. Research in the fruit fly, *Drosophila melanogaster*, has improved our understanding of how contact chemosensation influences vital behaviors due to the unparalleled genetic and neurobiological tools available in this organism. Recent studies, guided by the whole-brain fly connectome, have begun to unveil the neural underpinnings of complex and flexible behaviors. However, much remains unknown about the chemosensory mechanisms that encourage animals to prioritize one behavior over another.

One way that similar taste modalities can differentially drive behavior is through functional division by different chemosensory organs. The main peripheral taste organ in *Drosophila*, the labellum, contains the largest concentration of specialized gustatory receptor neurons (GRNs), housed in taste sensilla. ^{13,14} The fruit fly is equipped with many genes encoding transmembrane proteins that act largely as multi-subunit, ligand-gated ion channels, including gustatory receptors and ionotropic receptors (IRs). ^{14,15} Many of these are tuned to specific tastants and exhibit localized expression within sensory neurons with

specific functions. For example, neurons expressing specific sugar receptors Gr64f or Gr5a are classified as "sweet" GRNs that induce appetitive feeding, while neurons with receptors such as Gr66a or Gr33a are classified as "bitter" GRNs that elicit feeding avoidance. 14,16 These GRNs are located in the labellum as well as additional sensory organs where they can differentially impact feeding and egg-laying behaviors. 17,18 Female Drosophila need to make pivotal decisions about locations on which to feed or to lay eggs, and a complex mixture of chemical cues from plant hosts, microorganisms, and other flies allows females to assess potential costs and benefits to offspring. 3,19-21 Currently, chemosensation on the labellum has been largely tied to feeding behaviors, but the labellum touching an egglaying substrate is an established early step in the oviposition behavioral sequence, 22,23 and the role of chemosensation in this process remains largely unexplored.²⁴

While updating a comprehensive map of GRNs across the *Drosophila* labellum, we previously identified a unique subset of GRNs characterized by expression of *Ionotropic Receptor 94e (IR94e)* that did not overlap with any other population (sweet, bitter, water, or high-salt cells). These cells were minimally implicated in low sodium detection, ²⁵ leading us to believe that they, and the IR94e receptor itself, may have other roles. This work aims to elucidate the role of IR94e sensory neurons in behavior, find additional ligands that activate IR94e neurons, and identify the necessity of *IR94e* in a behavioral context. Using direct



¹Department of Biology, The University of Vermont, Burlington, VT 05405, USA

²Department of Zoology, Life Sciences Institute and Djavad Mowafaghian Centre for Brain Health, The University of British Columbia, Vancouver, BC V6T 1Z3, Canada

³Lead contact

^{*}Correspondence: michael.gordon@ubc.ca (M.D.G.), molly.stanley@uvm.edu (M.S.) https://doi.org/10.1016/j.celrep.2024.114625





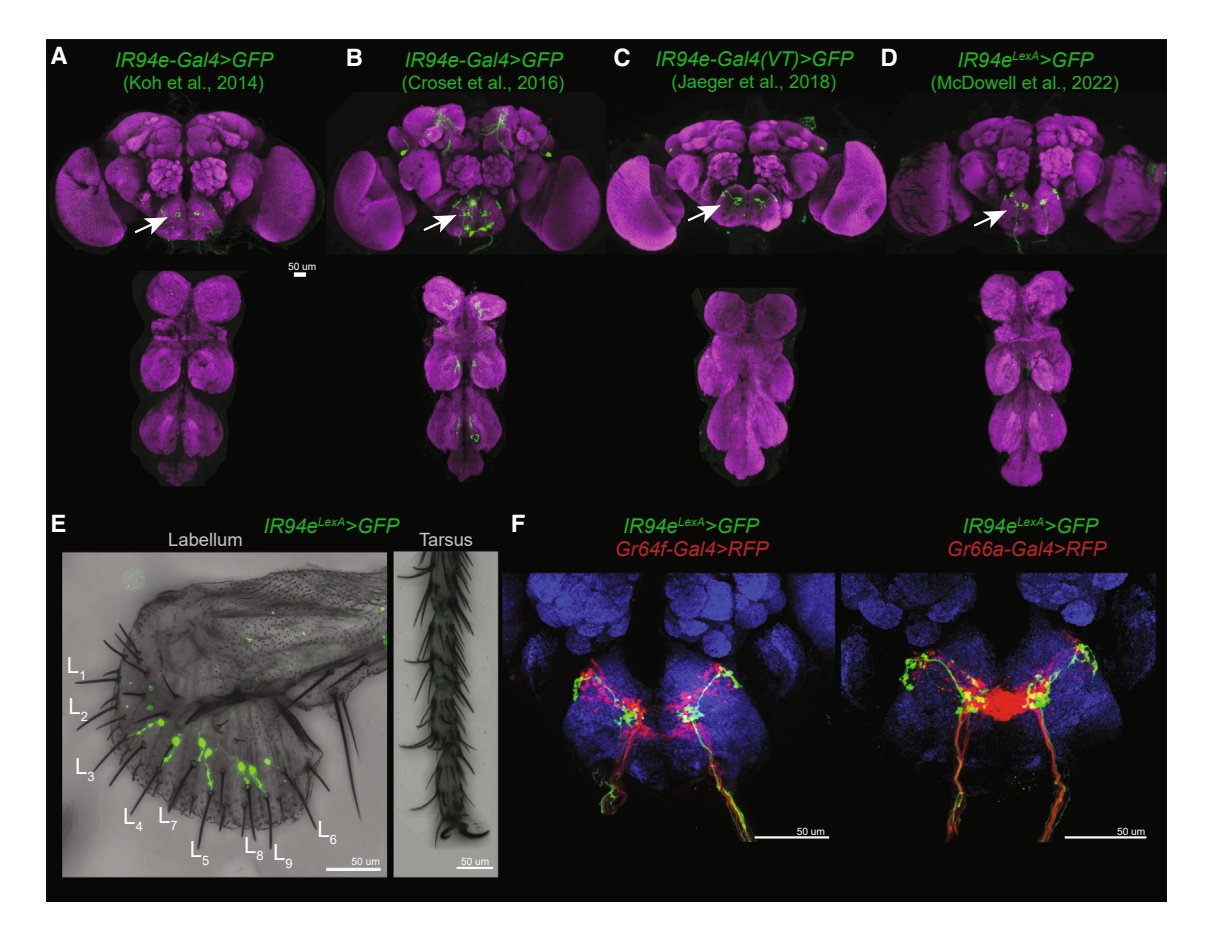


Figure 1. IR94e drivers label L-type GRNs with a unique projection pattern in the SEZ

(A–D) Indicated driver lines expressing *UAS* or *LexAop mCD8*::*GFP*. Brain and VNC with neuropil and GFP staining in mated females. Arrows indicate the specific pattern of axon terminals in the SEZ from labellar GRNs that is common across all lines.

- (E) IR94e^{Levil} driving GFP expression in the labellum, labeling one GRN in each of the L-type sensilla. No GFP expression in the tarsus.
- (F) IR94e GRNs expressing GFP and canonical "sweet" GRNs (Gr64f, left) or "bitter" GRNs (Gr66a, right) expressing RFP. Scale bars, 50 µm.

neuronal activation, *in vivo* calcium imaging, and *IR94e* mutants, we found that an IR94e receptor complex is responsible for both mild feeding aversion and increased oviposition on substances containing amino acids. Our findings regarding this unique set of labellum-specific taste neurons provide a pathway where the same set of cells on one organ can reciprocally impact two key behaviors.

RESULTS

Taste cells expressing *IR94*e are located in labellar L-type sensilla

Currently, there are three Gal4 driver lines for *IR94e* and one *IR94e* LexA knockin line (Figures 1A-1D). The initial *IR94e-Gal4* transcriptional reporter aimed to maximize fidelity by fusing the 5' and 3' flanking regions of the gene to the 5' and 3' ends of the *Gal4* sequence, and drives expression weakly and specifically in labellar cells that project to the suboesophageal zone (SEZ) in a pattern reminiscent of sweet GRNs²⁶ (Figure 1A). A second *IR94e-Gal4*, generated by targeting the entire 5' intergenic region, leads to strong expression in the same SEZ

pattern. However, it also strongly labels other SEZ neurons, higher-order neurons, and the ventral nerve cord (VNC)^{27,28} (Figure 1B). Although we do not know which cells this Gal4 line labels in the VNC, staining in the thoracic ganglia suggests they are associated with the legs, not the abdomen.²⁹

While previously mapping taste cells across the labellum, we identified Vienna Tiles line VT046252-Gal4 with Gal4 expression under the control of a genomic region upstream of the IR94e locus,²⁵ which we will refer to as IR94e-Gal4(VT). This line drives strong expression in the same SEZ pattern as the other two lines, with no VNC expression, but there is weak expression in two higher-order neurons (Figure 1C). We recently generated a knockin line with LexA::p65 inserted into the coding region of IR94e (IR94e^{LexA})³⁰ and now describe the expression patterns for this new driver line. IR94e^{LexA} drives strong and specific expression only in the consistent SEZ pattern in the brain, with no VNC expression (Figure 1D). One previous report of the IR94e-Gal4 with VNC expression suggested possible sexual dimorphism.²⁸ However, we found similar expression patterns in males, with clear SEZ expression from labellar cells in each line (Figures S1A-S1D).

Article



We previously demonstrated with IR94e-Gal4(VT) that the SEZ pattern was due to a single GRN in each L-type sensilla that did not overlap with "sweet," "bitter," "high-salt," or "water" cells.²⁵ We confirmed that the IR94e^{LexA} line also labels one GRN in each L-type sensillum on the labellum with no expression in tarsal GRNs (Figure 1E). The patterns from driver lines cannot completely rule out the expression of IR94e in other chemosensory cells, but transcriptomics from Fly Cell Atlas³¹ and a recent analysis of IR expression across tissues in Drosophilids³² similarly shows IR94e expression in labellar but not tarsal cells (Figure S3D). Co-labeling confirmed that the cells labeled by IR94e^{LexA} and the other Gal4 drivers overlap on the labellum and in their SEZ projection pattern (Figures S1E-S1J), although GFP driven by IR94e^{LexA} was not always visible in all nine GRNs, and the Koh et al.²⁶ Gal4 driver labeled an even smaller number of GRNs when co-expressed (Figures S1I and S1J). We conclude that these lines label the same set of labellar taste cells with some variability in coverage and that the IR94e^{LexA} and IR94e-Gal4(VT) driver lines offer strong yet specific expression in this set of L-type "IR94e GRNs."

Based on the SEZ projection pattern, IR94e was originally speculated to be expressed within sweet taste cells. ²⁶ However, we previously showed that IR94e GRNs are separate from other groups on the labellum, ²⁵ and here we show that the SEZ projection patterns are also unique: IR94e axon terminals cluster in a medial lateral space within but not overlapping with the sweet terminals, and near the lateral region of bitter terminals (Figure 1F). The anatomical segregation of sweet and bitter projections is the first step of neural processing for these opposing taste modalities, ¹⁶ and IR94e GRNs terminating in a unique location may also indicate a distinct function for these taste cells.

IR94e GRN activation leads to mild feeding aversion

To establish whether IR94e GRN activation leads to changes in feeding behavior, such as a change in preference or the number of interactions with a food source, we used optogenetics and chemogenetics to directly activate IR94e sensory neurons in various feeding assays. CsChrimson is a red-light-gated cation channel that requires prefeeding of flies with all-trans-retinal (ATR) to function. Therefore, in all optogenetic experiments, flies of the same genotype but without ATR prefeeding are used as controls. Mated females were used in all behavioral experiments except where indicated. We started our optogenetic investigation by examining an initial feeding behavior triggered by appetitive taste cues, known as the proboscis extension response (PER).³³ Optogenetic activation of sweet GRNs is sufficient to induce PER in the absence of any physical taste stimulus³⁴⁻³⁶ (Figure S2A), while activation of bitter GRNs is sufficient to inhibit the PER to a sugar stimulus³⁷ (Figure S2C). Optogenetic activation of IR94e GRNs did not induce any PER (Figure S2B) but significantly reduced the PER to 100 mM sucrose in two of the four driver lines (Figure 2A). This suggests that IR94e GRNs may be mildly aversive, as the driver lines consistently labeling all IR94e GRNs (IR94e-Gal(VT) and IR94e-Gal4²⁷) showed an effect, while lines with more variability did not (IR94eLexA and IR94e-Gal4²⁶). Given this inconsistency, we turned to other behavioral assays to confirm whether these taste cells lead to feeding aversion.

To investigate the impact of IR94e GRN activation on freely feeding flies, we performed optogenetic binary-choice experiments with the same concentration of sucrose as a food source on each side, and one side triggering a red light to induce GRN activation during the duration of the fly's interaction with that food.^{38,39} It was shown previously that most interactions with the presented food sources are "sips" or "licks"-involving food ingestion-but some may be shorter "tastings" with the tarsi. 40,41 In this assay, flies with active CsChrimson channels in IR94e GRNs using both the IR94e-Gal4(VT) and IR94e^{LexA} drivers showed a clear preference for sucrose without the red light (Figure 2B). The preference index was calculated from the number of interactions with each sucrose food source. Comparing the number of interactions suggests that flies are both avoiding the light-triggering sucrose and interacting more with the non-triggering sucrose (Figure 2B). We also tested whether this phenotype exists in males and found a strong preference for sucrose without the light (Figure S2D).

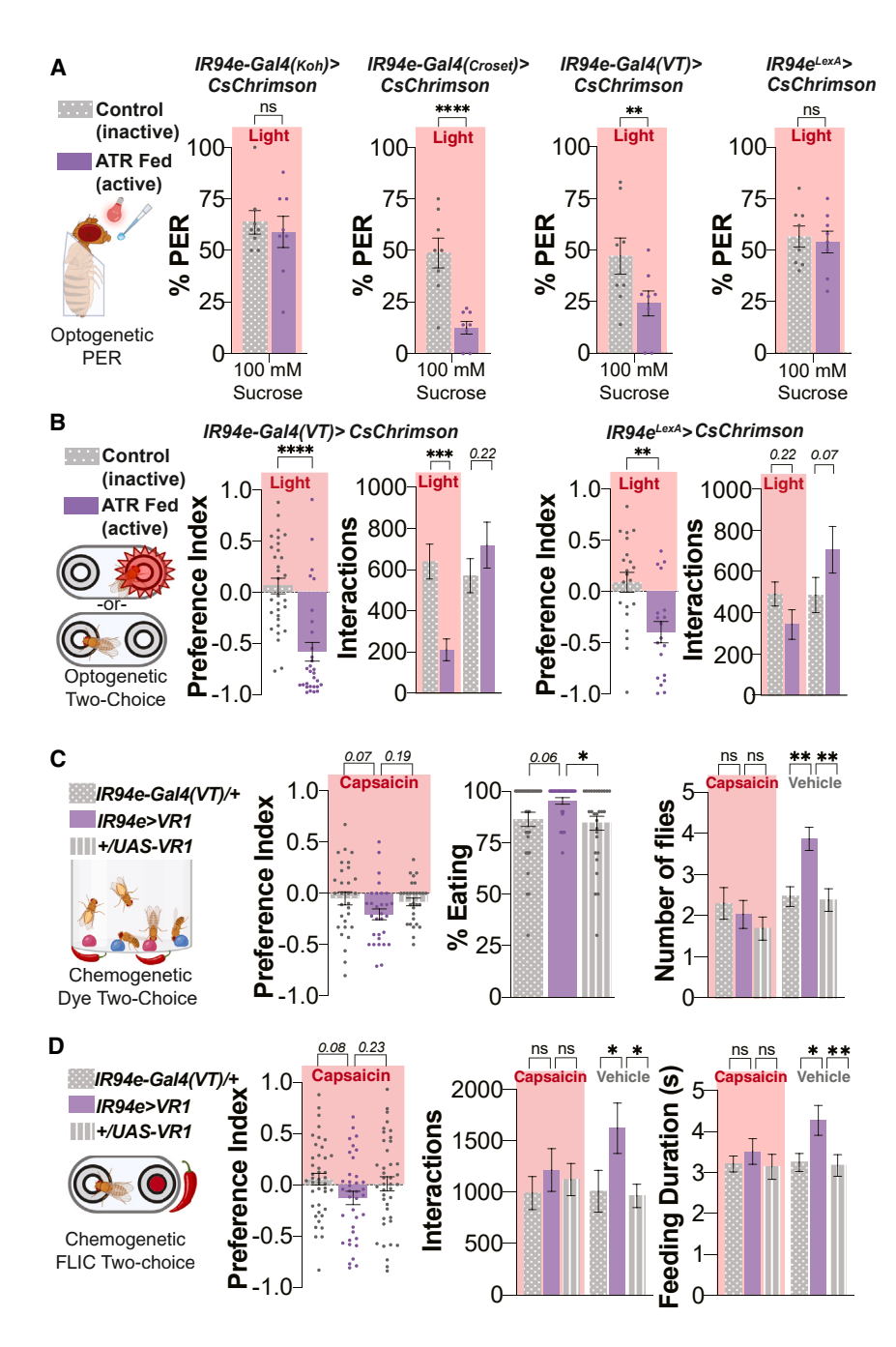
One potential caveat of the optogenetic binary-choice assay is that the light will be triggered whether flies taste the solution with their tarsus or labellum. Therefore, we used chemogenetics that require contact of the labellar IR94e GRNs with a substrate for activation. The IR94e-Gal4(VT) line was used to express VR1 (TRPV1), an ion channel gated by capsaicin or noxious heat. 42 This channel is not normally expressed in Drosophila taste cells, so it can be used as a chemogenetic tool to activate taste cells with a "neutral" chemical stimulus to determine the behavioral valence of GRNs. 16 Using a dye-based binary-choice assay, we first reproduced previous findings to show that expressing VR1 in Gr64f-sweet taste cells generated a positive preference for capsaicin compared to genetic controls, with more flies consuming capsaicin and fewer consuming vehicle (Figure S2E). Expressing VR1 in Gr66a-bitter taste cells showed the opposite result from sweet activation, as expected (Figure S2F). The number of flies eating any option in this assay was strongly increased with sweet cell activation (Figure S2E) and mildly lower with bitter cell activation, although this result did not achieve statistical significance (Figure S2F). Repeating the experiment with IR94e activation revealed a weak negative preference index for capsaicin that also did not achieve statistical significance compared to genetic controls (Figure 2C). The number of flies consuming the vehicle option was significantly higher, indicating a clear interest in the non-capsaicin option. Unexpectedly, the number of flies consuming either option in this assay was increased, despite the mildly aversive preference (Figure 2C). To investigate this phenotype further, we repeated this experiment in the fly liquid-food interaction counter (FLIC)⁴⁰ to record each food interaction and the feeding durations. We found a similarly mild and statistically insignificant preference index away from the capsaicin, but flies interacted significantly more with the vehicle option and for longer durations (Figure 2D).

In summary, although several experiments produced only trends that did not reach statistical significance, taken together our results suggest that IR94e activation leads to a mild feeding aversion.

IR94e GRN activation stimulates egg laying

To determine whether IR94e GRNs may be involved in other behaviors that rely on chemosensation, we turned to the





D. melanogaster whole-brain connectome in which every neuron and synapse from one female brain has been fully reconstructed with predicted neurotransmitters. 4-6,43,44 IR94e and other GRNs were previously identified in the connectome, where they were found to synapse with local interneurons and putative taste projection neurons (TPNs). 35,37,45-47 Using FlyWire⁵ (version 630), we identified IR94e GRNs and performed morphological clustering to show that these neurons are anatomically distinct from Gr64f "sweet" GRNs (Figure S3A). 48,49 We next identified a link to oviposition by observing that IR94e GRNs synapse onto projection neurons connecting to oviposition descending neurons

Figure 2. IR94e GRN activation leads to mild feeding aversion

(A) Optogenetic activation of IR94e GRNs with labellar sucrose stimulation in indicated driver lines. n = 8-9 groups of 6–10 flies per group, ATR (all-trans-retinal fed for active channels).

(B) Optogenetic activation of IR94e GRNs in a two-choice chamber with 100 mM sucrose on both sides; one side triggers light with contact. Preference index (left) from the number of interactions (right). n=30–31 flies (Gal4), n=19–21 flies (LexA). (C) Chemogenetic activation of IR94e GRNs using VR1 and 100 μ M capsaicin vs. vehicle (0.07% EtOH) in a dye-based, two-choice assay. Preference index (left), total percentage of flies eating any option (middle), and number of flies consuming capsaicin vs. vehicle (right). n=29–30 groups of 10 flies.

(D) Chemogenetic activation of IR94e GRNs in an FLIC two-choice assay. Preference index (left) from number of interactions with each side (middle), and feeding durations (right). n=37-42 flies per genotype. All mated females.

All data plotted as mean \pm SEM. ns, p > 0.25; trending p values indicated. *p < 0.05, **p < 0.01, ****p < 0.001, ****p < 0.001 by two-way ANOVA with Sidak's post test (A, number of flies, interactions, feeding duration), one-way ANOVA with Dunnett's post test (C and D, preference index, % eating), or t test (B, preference index). Assay graphics created with Biorender.com.

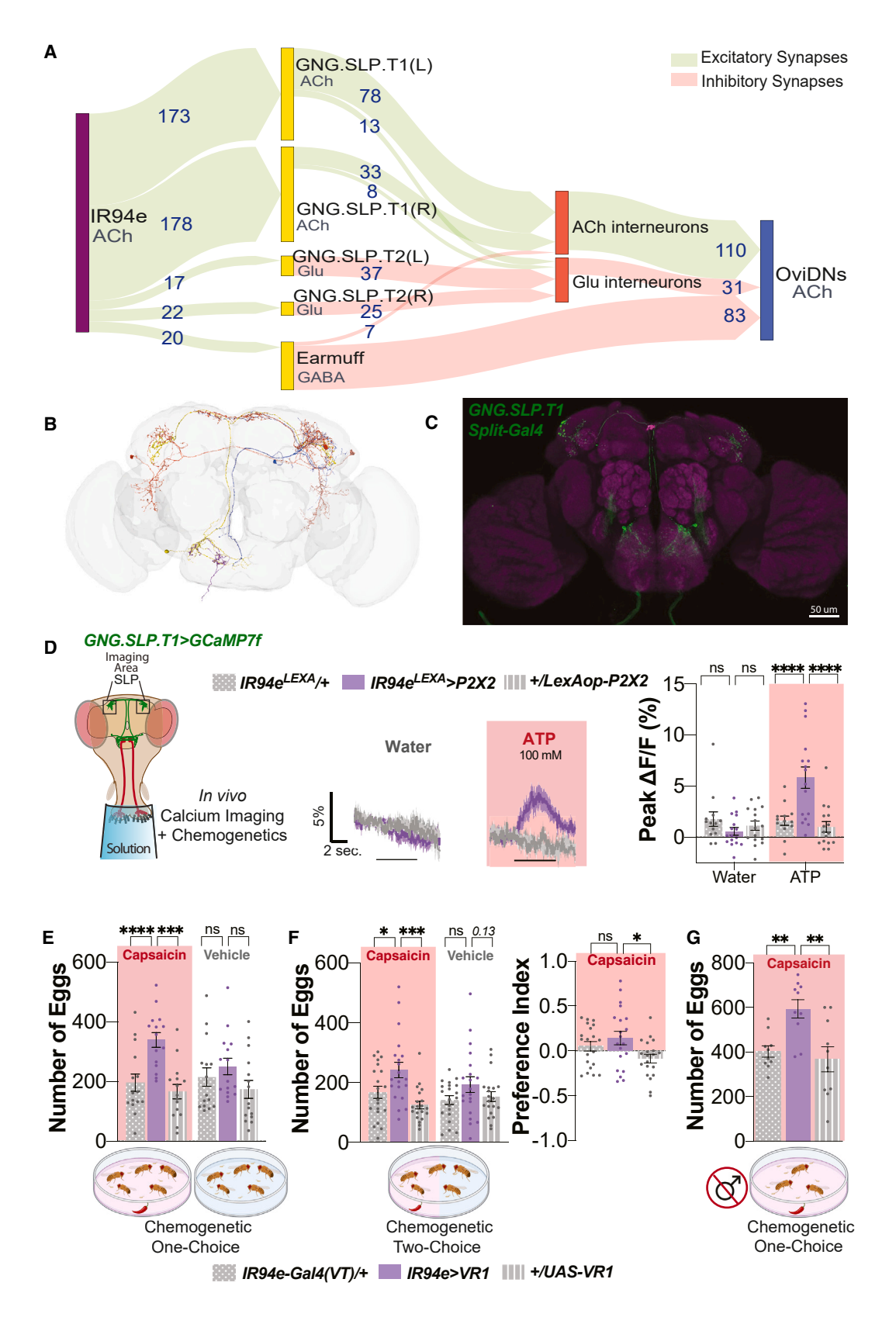
(OviDNs), either directly or through one interneuron (Figures 3A and 3B). One set of projection neurons, referred to as GNG.SLP.T1 (L) for left hemisphere and (R) for right hemisphere (Figure S3B), have the highest synapse numbers with IR94e GRNs. These TPNs receive excitatory input from IR94e GRNs and form excitatory synapses with third-order cholinergic interneurons that connect to OviDNs as well as a small number of synapses with glutamatergic interneurons that are predicted to inhibit OviDNs. Another set of TPNs, referred to as GNG.SLP.T2 (L) or (R), connect IR94e GRNs to OviDNs via two predicted inhibitory (glutamatergic) synapses, which

should derepress OviDN activity following IR94e stimulation. Finally, the TPN previously identified as Earmuff⁴⁵ (Figure S3B) connects IR94e GRNs to OviDNs via a predicted inhibitory pathway, albeit with very few synapses. Since OviDN neuronal activity is necessary and sufficient to induce egg laying,⁵⁰ we hypothesized that IR94e GRNs may impact oviposition.

Given the synaptic strength of each connection in these circuits, the putative TPNs most likely to be activated by IR94e GRNs are the GNG.SLP.T1 neurons, which are part of an excitatory circuit to the OviDNs. To confirm the existence of a functional synapse, we generated a split-Gal4 line 51,52

Cell ReportsArticle





(legend on next page)





(VT019729-AD; VT008484-DBD) that labels these projection neurons (Figure 3C). We chemogenetically activated IR94e GRNs by expressing LexAop-P2X2,53 an ATP-gated cation channel,54 under control of IR94e^{LexA} in flies that also had two copies of GCaMP7f driven by the split-Gal4 VT019729-AD; VT008484-DBD. Fluorescence was recorded in vivo from the projection neuron axon terminals in the superior lateral protocerebrum (SLP) in either hemisphere, while the labellum was stimulated with water (negative control) or 100 mM ATP (experimental solution). ATP produced a significant increase in the GNG.SLP.T1 calcium signal compared with the two control genotypes (Figure 3D). This confirms that IR94e GRNs functionally synapse onto downstream circuits that ultimately lead to the OviDNs in the connectome.

Based on these connectomic data, we used chemogenetics to test the hypothesis that IR94e activation increases egg laying. Flies expressing VR1 under control of IR94e-Gal4(VT) were allowed to lay eggs on an agar substrate containing either capsaicin or vehicle. We saw no difference between groups exposed to vehicle, but on capsaicin the activated group laid significantly more eggs compared to genetic controls (Figure 3E). To determine whether flies show a preference for laying eggs directly on a substrate that activates IR94e GRNs, we repeated this experiment in a two-choice manner with only half of the plate containing capsaicin. Again, we found that the number of eggs laid on capsaicin was significantly higher in the IR94e>VR1 group compared to both genetic controls, but the overall oviposition preference for capsaicin was very mild and only significant compared to one genetic control (Figure 3F). To confirm that the presence of males or IR94e activation in males does not influence this oviposition phenotype, we repeated this assay with the males removed prior to capsaicin exposure and found that IR94e>VR1 females still laid significantly more eggs than control genotypes (Figure 3G). To verify that this behavior was due to labellar chemosensation, we confirmed that females do not have any IR94e-positive neurons in the ovipositor (Figure S3C), agreeing with a recent report that IR94e mRNA is present in the labellum but not the ovipositor in D. melanogaster. 32 Single-cell transcriptomics from the Fly Cell Atlas³¹ further revealed no IR94e expression in female reproductive tissues, oenocytes, or male reproductive glands, although IR94e+ cells were found in the testis (late cyst cells and spermatocytes) (Figure S3D). While the expression of IR94e in the testis is intriguing, this would not impact the oviposition phenotype (Figure 3G). Overall, these

results indicate that labellar IR94e GRN activity in females increases egg laying, consistent with the predicted synaptic connections to OviDNs.

IR94e GRNs respond to amino acids through an IR

Next, we sought to identify candidate molecules that stimulate IR94e GRNs. Using in vivo calcium imaging, we stimulated the labellum with a liquid solution and simultaneously recorded the change in GCaMP6f fluorescence in the axon terminals of IR94e GRNs in the SEZ (Figure 4A). Previously, we reported that IR94e GRNs do not respond to sucrose (sweet), lobeline (bitter), water, or high concentrations of salts, but do have a small response to low Na⁺. 25 We suspected that other, unidentified ligands may stimulate these taste cells more robustly. A screen of various compounds including pheromones, fatty acids, carboxylic acids, and alkaline solutions produced mostly negative results (Figure 4A). Tryptone, a digestion of the casein protein resulting in a mix of amino acids (AAs), was the only solution to produce a strong response in IR94e GRNs (Figure 4A). Yeast extract also contains AAs along with other types of molecules, but in concentrations that differ from tryptone. Glutamate is the most abundant AA in tryptone, so we tested two forms of glutamate and eight other AAs found in tryptone at various levels. Acidic AAs, glutamate and aspartate, led to significant increases in IR94e calcium compared with water, while others did not (Figure 4A). Notably, individual flies occasionally had large responses to some AAs, but not as consistently as glutamate. Glutamic acid is only soluble in water at low concentrations, so it is more commonly used in the form of monosodium glutamate (Na+ glutamate, or MSG) or monopotassium glutamate (K⁺ glutamate, or MPG). Given these neurons have a small Na⁺ response but no K⁺ response,²⁵ we used both salt forms of glutamate and found similar responses (Figure 4A). We also directly tested the same concentrations of NaCl, Na+ glutamate, KCl, and K+ glutamate and found that the glutamate form stimulated IR94e GRNs significantly more than the chloride salts (Figure S4A). Glutamic acid without salt also produced a significant response in IR94e GRNs at the maximum water solubility, similar to K⁺ glutamate at the same concentration (Figure S4B), and there were dosedependent responses to K⁺ glutamate (Figure S4C). A representative heatmap shows a uniform response across IR94e projections (Figure S4D).

Figure 3. IR94e GRN activation leads to an increase in egg laying

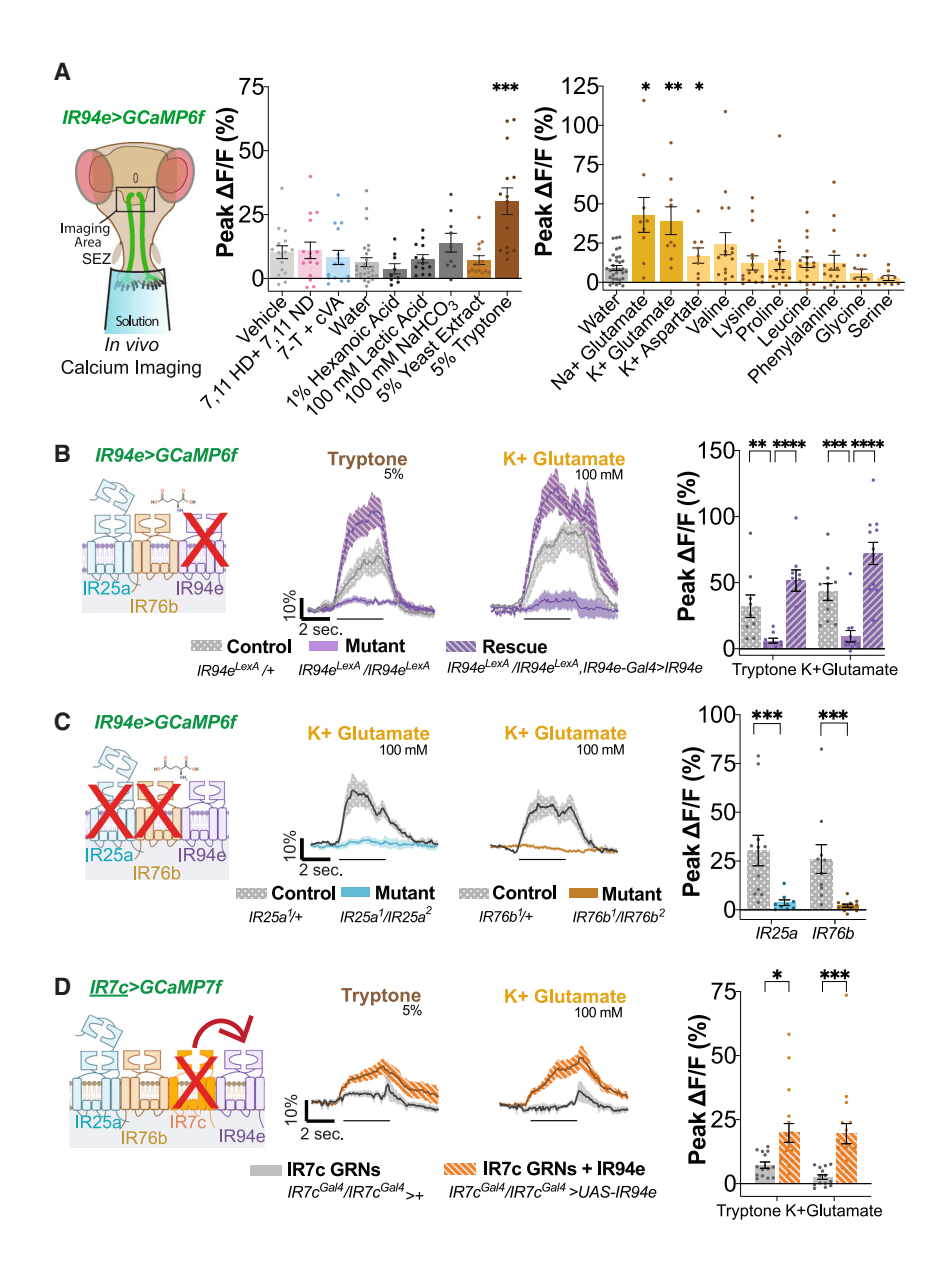
(A) Connectomic analysis in FlyWire v630: IR94e GRNs synapse onto putative taste projection neurons to connect with oviposition descending neurons (OviDNs). Predicted neurotransmitter and synapse numbers are displayed.

- (B) Neurons in the excitatory circuit connecting IR94e GRNs to OviDNs: IR94e,= purple; GNG.SLP.T1, yellow; interneuron, red; OviDN, blue.
- (C) GNG.SLP.T1 split-Gal4 (VT019729-AD;VT008484-DBD) driving UAS-Chrimson(YFP). Scale bar, 50 μ m.
- (D) GNG.SLP.T1 split-Gal4 driving two copies of UAS-GCaMP7f; calcium responses recorded during chemogenetic activation of IR94e GRNs with ATP (IR94e>P2X2), n = 13-16 flies per group. Imaging from the left and right SLP balanced in each group; black lines under curves indicate when the stimulus is on the
- (E) Egg laying during chemogenetic activation of IR94e GRNs with capsaicin (IR94e>VR1) in flies given one option (100 μM capsaicin or vehicle [0.07% EtOH]). n = 16 groups of 12 females and 8 males.
- (F) Same as (E) but in a two-choice egg-laying assay (100 μM capsaicin vs. vehicle). Total number of eggs on each substrate (left), egg-laying preference index (right), n = 20 groups of 12 females and 8 males.
- (G) Chemogenetic one-choice egg-laying assay with males removed before capsaicin exposure. n = 10 groups of 12 females.
- All data plotted as mean \pm SEM. ns, p > 0.25; trending p values indicated. *p < 0.05, **p < 0.01, ***p < 0.001, ***p < 0.0001 by two-way (D) or one-way (E-G) ANOVA with Dunnett's post test. Oviposition graphics created with Biorender.com.

6

Article





After establishing that IR94e GRNs respond to certain AAs, we determined which receptors are involved by repeating the in vivo calcium imaging in flies with mutations in candidate IR genes. IR94e codes for a transmembrane protein that is part of the ionotropic family of chemosensory receptors. 26,28,55-57 Flies with homozygous IR94e^{LexA} knockin alleles showed a significant loss of tryptone, K+ glutamate (Figure 4B), glutamic acid, and Na⁺ glutamate (Figure S4E) responses that could be rescued with expression of UAS-IR94e using IR94e-Gal4(VT). Notably, the responses were even higher with IR94e rescue, suggesting that the rescue may lead to expression that is higher than the heterozygous controls. These data further support the role of the IR94e receptor in detecting these ligands. We tested whether this phenotype persists in male flies and found that calcium responses in controls were minimal, but the rescue showed notable responses, which may again suggest potentially higher

Figure 4. IR94e GRNs are activated by amino acids through an IR complex

(A) In vivo calcium imaging of GCaMP6f in subesophageal zone (SEZ) axon terminals with labellar stimulation. Ligand screen, n = 9-16 flies per group, only 3-6 chemicals presented to each fly, plotted together for visualization. One-way ANOVA with post tests comparing each chemical to the negative control in that set (water or vehicle for pheromones). Water controls for the group with aspartate and valine differed slightly but are plotted together for visualization (valine p = 0.3). (B) Calcium imaging of IR94e GRNs in heterozygous controls, homozygous IR94e mutants, or IR94e mutants with IR94e(VT)Gal4 driving UAS-IR94e (rescue). Fluorescent curves over time (left) and peak changes in fluorescence (right), n = 9-13flies per group.

(C) Calcium imaging of IR94e GRNs in heterozygous controls or homozygous mutants. Fluorescent curves over time (left) and peak changes in fluorescence (right), n = 9-11 flies per group.

(D) Calcium imaging of "high-salt" IR7c GRNs with GCaMP7f, IR7c mutant background, with IR7c-Gal4 driving UAS-IR94e. Fluorescent curves over time (left) and peak changes in fluorescence (right), n = 14-17 flies per group.

Black lines under curves indicate when the stimulus is on the labellum. All in mated females. All data plotted as mean ± SEM. ns, not significant; trending p values are shown. *p < 0.05, **p < 0.01, ***p < 0.001, ****p < 0.0001 by one-way ANOVA with Dunnett's post test (A), two-way ANOVA with Sidak's post test (B and D), or unpaired t test (C). Receptor graphics created with Biorender.com.

expression in the rescue (Figure S4F). We included 100 mM NaCl in this panel to determine whether IR94e also plays a role in detecting low salt in these cells²⁵ and found no significant loss in IR94e mutants and no exaggerated response with IR94e rescue (Figures S4E and S4F). Thus, we conclude that IR94e is more involved in detecting glutamate than Na+.

Since IR94e is expressed in a small and specific set of GRNs, we hypothesized that it likely acts as a "tuning receptor" that works with more broadly expressed co-receptors, IR25a and IR76b. This type of receptor complex has been identified in other GRNs. 30,58,59 The K⁺ glutamate calcium response in IR94e GRNs was completely abolished in flies with homozygous mutations in IR25a or IR76b (Figure 4C). These results suggest that IR25a, IR76b, and IR94e are all necessary for detecting this ligand. To test for sufficiency, we utilized another set of GRNs known to have IR25a and IR76b working with a different tuning receptor, IR7c, for the detection of high salt.30 With an IR7c mutant background to abolish any salt detection, we introduced UAS-IR94e and found that this generated small but significant responses to both tryptone and K⁺ glutamate (Figure 4D). This indicates that IR94e expression in GRNs that contain IR co-receptors is sufficient to confer AA sensitivity.



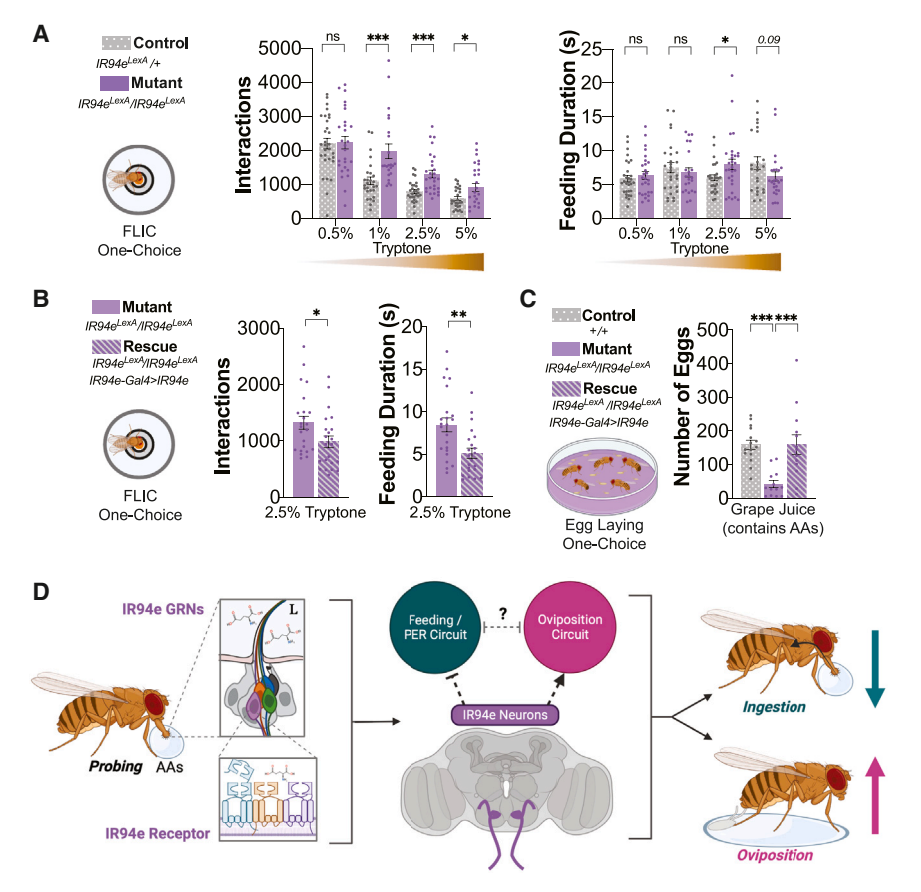


Figure 5. IR94e mutants show altered feeding and egg laying on amino acids

(A and B) FLIC one-choice assay in mated females in (A) controls and IR94e mutants, n=26-33 flies per group, or (B) mutant and rescue flies (IR94e(VT)Gal4) driving expression of UAS-IR94e), n=22-23 flies per group.

(C) One-choice egg-laying assay on grape plates in control, mutant, and rescue flies, n=13-15 groups of 12 females and 8 males.

(D) Model for IR94e GRNs reciprocally impacting feeding and egg-laying behavior. One IR94e GRN in each L-type sensilla on the labellum (purple cell) responds when flies come in contact with certain AAs while probing substrates through the IR94e receptor. IR94e neurons synapse with projection neurons to ultimately inhibit feeding and increase egg laying. Unknown details including interactions between downstream circuits are represented by dotted lines and a question mark. Assay graphics and model created with Biorender.com.

All data in (A)–(C) plotted as mean \pm SEM. ns, not significant; $^*p < 0.05$, $^{**}p < 0.01$, $^{***}p < 0.001$, by two-way ANOVA with Sidak's post test (A), unpaired t test (B), or one-way ANOVA with Dunnett's post test (C).

Loss of *IR94*e impacts feeding and egg laying on amino acid solutions

To connect our calcium imaging results back to GRN-specific behavior, we investigated tryptone feeding in flies with homozygous IR94e^{LexA} knockin alleles to disrupt AA detection specifically in the IR94e GRNs. We used the FLIC assay to quantify the number of interactions and feeding durations on tryptone as a metric of interest and intake. IR94e mutants had significantly more interactions with a tryptone solution at concentrations of 1% or higher (Figure 5A). In parallel, there was a significant increase in the feeding duration on 2.5% tryptone (Figure 5A). We repeated this experiment with water, sucrose, or 2.5% tryptone and found that IR94e mutation only impacted the feeding responses to tryptone, significantly increasing both interactions and feeding durations (Figure S5A). This indicates that IR94e mutants are not generally more thirsty or hungry. Expressing UAS-IR94e in a rescue experiment significantly reduced tryptone interactions and feeding durations compared to IR94e mutants (Figure 5B). We tested for this IR94e mutant phenotype in males and found a similar increase in tryptone interactions but no change in feeding durations (Figure S5B). We further repeated the 2.5% tryptone FLIC experiment in mated females with an opto-lid to acutely silence IR94e GRNs using GtACR1, a green-light-gated anion channel. 60 Flies fed ATR with active channels showed a significant increase in the feeding duration on tryptone and a small statistical trend toward increased interactions (Figure S5C), in the same direction

as the *IR94e* mutants. These results suggest that IR94e normally limits tryptone ingestion.

To examine the impact of IR94e mutation on oviposition behavior, we used

grape juice, a common egg-laying substrate that naturally contains an abundance of AAs, including glutamate. ^{61,62} We found that *IR94e* mutants laid significantly fewer eggs on grape juice while *UAS-IR94e* expression significantly restored egg numbers (Figure 5C). We supplemented the grape juice with additional glutamate in the form of glutamic acid to avoid any impact of salt ions and obtained results similar to those of grape juice alone (Figure S5D). These results suggest that *IR94e* is normally sensing chemicals in this assay to encourage egg laying.

Based on our results, we propose a model (Figure 5D) in which IR94e GRNs in L-type sensilla on the labellum detect AAs while mated females are probing the environment to reciprocally discourage feeding on that substrate and encourage egg laying on or near the substrate.

DISCUSSION

Understanding how nervous systems enable animals to perform advantageous behaviors in response to their environment has various implications, from controlling invasive pest species to better understanding human health. In this study, we provide evidence that one small set of taste cells on a single chemosensory organ can differentially impact two fundamental behaviors, providing a key addition to a growing body of literature on how chemical cues can help animals prioritize behaviors based on the environment.

Article



Behavioral impact of IR94e GRN activation

The Drosophila whole-brain connectome has facilitated the description of a complete PER circuit.³⁵ Applying a leaky integrate-and-fire model to this circuit predicted that IR94e GRNs would inhibit PER,³⁷ which was supported by the observation that IR94e activation inhibited sucrose PER (with 50 mM).37 The results from our PER experiments (with 100 mM sucrose) and additional feeding assays provide further support for this conclusion (Figures 2A-2D). We also found that IR94e GRNs have a negative feeding valence in males (Figure S2D), suggesting that these sensory neurons directly act to inhibit feeding circuits. Previously, we found that low salt attraction was reduced by chronic, but not conditional, silencing of IR94e GRNs,²⁵ which made the role of IR94e GRNs in salt feeding somewhat difficult to discern. The chronic silencing results suggested that these cells play a role in attractive feeding, but metabolic effects or compensation from long-term silencing may have occurred and potentially shifted the impact of IR94e GRNs on feeding under specific conditions. Nonetheless, it is now clear that both IR94e and highsalt GRNs can contribute to feeding aversion from chemicals detected by the L-type sensilla on the fly labellum. In contrast to bitter GRNs, which provide strong and consistent behavioral aversion, we previously found that the aversiveness of highsalt GRNs depends on internal state. 25,30 It appears that IR94e-mediated feeding aversion is even milder but may reduce food interest to the extent that exploration and other behaviors can become a priority over feeding, perhaps also based on internal state.

In this study, the connectome provided a potential link between IR94e GRNs and egg-laying behaviors that was confirmed experimentally. Detailed descriptions of the egglaying sequence show that proboscis extension and the labellum touching the substrate are early essential steps, 21-23 and one study previously implicated labellar GRNs in the oviposition preference for acetic acid.²⁴ Our results provide a labellar-specific cell type and ligand-receptor interaction for another class of chemicals in this egg-laying process. Another essential behavior involving chemosensation is mating,63 and a subset of bitter GRNs on the labellum can detect pheromones to guide male mating behaviors.⁶⁴ A recent description of cVa olfactory circuits for mating used connectomics to identify another set of neurons that receive inputs from IR94e GRNs and connect to circuits controlling female receptivity.¹¹ Interestingly, direct activation of IR94e GRNs did not increase mating, but co-activation of IR94e GRNs plus a specific set of olfactory projection neurons did. The IR94e-Gal4 with broader expression was likely used in these experiments (Figure 1B),11 making them more difficult to interpret. However, if labellar IR94e GRN activity can increase female receptivity in the presence of sufficient cVA, 11 these neurons could promote both copulation and oviposition in females.

The IR94e-mediated inhibition of feeding and enhancement of egg laying may act independently via parallel circuits identified for PER^{35,37} and oviposition (Figures 3A and 3B). However, additional reciprocal inhibition could occur between downstream feeding and oviposition circuits to influence these competing behaviors more generally (Figure 5D). Other chemosensory signals (sour and bitter) can similarly encourage oviposition while producing positional avoidance, 18,24 and the reverse is true for sucrose in certain contexts. 17,21 Sensory signals that elicit egg laying, in particular, may promote opposing positional or feeding behaviors to encourage oviposition on ideal substrates. Future work can use the connectome as a guide to determine whether the brain processes these cues as competing priorities or whether the activation of one behavioral circuit can reduce the saliency of sensory cues for other behaviors.

An IR94e ligand-receptor complex

This work contributes to our understanding of AA taste. While mammalian AA taste research has largely focused on "umami" taste cells that express T1R1/T1R3,65 humans report that individual AAs taste "sweet," "bitter," "savory," or a combination of these, 66 and there is evidence that AAs can also activate bitter and sweet receptors. 67,68 In addition, the loss of T1R1/T1R3 does not fully eliminate neural and behavioral responses to AAs, suggesting a combinatorial taste system requiring multiple cell types and receptors. ^{69–72} In *Drosophila*, yeast was previously found to activate GRNs that express IR76b.73 We now know that this population includes numerous taste cells of various types, including IR94e GRNs, and it is likely that these cells and others all respond to food sources containing AAs. More recent work has shown that the broadly expressed co-receptors IR25a and IR76b are required for individual AA detection in sweet and bitter GRNs,⁵⁹ which agrees with our findings for IR94e GRNs (Figure 4C). However, tip recordings performed in this previous study did not reveal significant activation of L-type GRNs by glutamate, and they did not see any change in AA-induced action potentials from L-type sensilla after expressing pro-apoptotic genes in IR94e GRNs using the less-specific driver line (Figure 1B).⁵⁹ It is unclear why glutamate activation was not detected by electrophysiology, but testing only one sensillum (L6) or using a lower concentration of glutamic acid (25 mM) are potential explanations, as we saw only a minimal calcium response with double that concentration (50 mM) (Figure S4B). Regardless, tryptone, a more complex mix of AAs, also activated IR94e GRNs in our experiments, with IR94e being necessary and sufficient for its detection. Taken together, AA taste in flies appears to involve three different cell types on the labellum with at least three different receptors that allow for a range of behavioral responses to distinct chemicals, ⁵⁹ demonstrating complexities comparable to those of mammalian AA taste. 69 Interestingly, the fact that IR94e seems particularly tuned to glutamate also resembles mammalian T1R1/T1R3 responses.74

We hypothesize that the narrowly expressed IR94e may act as a tuning receptor to form a complex with broadly expressed IRs (IR25a, IR76b), but additional structural and functional confirmation is needed. The cooperation between IRs agrees with what is known for salt receptors in high-salt cells³⁰ and sweet cells,⁵⁸ and AA receptors in bitter cells that use IR51b.59 IRs are ancestrally related to mammalian ionotropic glutamate receptors but appear to have largely lost their glutamate binding domains. 55,56 Therefore, we were surprised to find that glutamate was a ligand. A recent study found that touching male Drosophila genitalia directly to the female labellum activates IR94e GRNs to a similar extent as low Na⁺. 11 However, the specific chemosensory cues on the genitalia were not identified. We did not see any response to a mix of male and female pheromones (Figure 4A), but other





cuticular chemicals may activate these cells, and perhaps a synergistic activation is possible with a combination of cues. With three identified sources of chemical ligands to date (AAs, low Na⁺, and male genitalia), the role of IR94e GRNs appears to be multifaceted.

Connections between IR94e receptors, ligands, and behavior

AAs, particularly glutamate, are the ligands showing the strongest activation of IR94e GRNs thus far, and we found that both feeding and egg laying on solutions containing AAs were altered in IR94e mutants and rescued with re-expression of IR94e (Figures 5A-5C). Protein and AA feeding increases in mated females, likely to support the nutritional demands of egg development.^{75–78} The presence of AAs, usually tested in the form of yeast, can both promote oviposition and support larval development,^{3,79} and a possible ethological implication of our results is that adults may not want to consume nutrients in the same area where their offspring will develop to reduce competition. The specific role of glutamate in this process is unclear: it may support specific nutrient needs, but, as one of the most abundant AAs in nature, it may also simply act as a signal for protein. 80,81 In addition, the aversive IR94e feeding phenotype in males may be due to their reduced AA needs, but we cannot rule out the possibility that IR94e GRN activation may impact other behaviors in males, such as conspecific communication. The AA calcium responses in males also appeared to be lower than those in mated females (Figures S4E and S4F). This could represent sexual dimorphism related to the flexible protein needs in females, but additional research is needed to uncover how biological sex impacts GRNs.

Future research can also determine whether IR94e responses to AAs and their behavioral output are modulated by internal needs. Activation of IR76b-expressing labellar GRNs by yeast was significantly enhanced with protein deprivation but not by mating, suggesting that internal state alterations by nutrition and reproduction may act differently on circuitry that connects AA sensing to feeding. A mixture of three specific AAs (serine, phenylalanine, and threonine) was found to activate sweet GRNs only after exposure to a low-protein diet, further suggesting that labellar GRN sensitivity to AAs can change in response to nutritional conditions. Two possibilities for modulation in our proposed model (Figure 5D) are that primary IR94e GRN output may be directly altered by internal state to differentially trigger postsynaptic circuits or that internal state may act on downstream neurons in feeding and/or oviposition circuits to allow for behavioral flexibility.

In conclusion, we find that the small population of IR94e GRNs on the *Drosophila* labellum act to simultaneously encourage oviposition and discourage feeding on AAs. Future work can further investigate the downstream neural circuitry of this phenomenon, potentially involving the mushroom body, ¹⁸ to understand more about how the nervous system performs this computation for competing behaviors across chemical cues.

Limitations of the study

The focus of this paper is on the role of IR94e in L-type sensilla of the *Drosophila* labella of mated females, but there may be additional phenotypes related to the *IR94e* gene beyond our current analysis. For example, the role of IR94e in males may be similarly

complex but more challenging to discern without a connectome. While we clearly see AA phenotypes with labellar IR94e, other chemicals may activate these GRNs. We therefore discourage referring to these cells as "amino acid" GRNs. In addition, although there are clear correlations between GCaMP signals and action potentials, ⁸³ calcium imaging does not directly assay neuronal activity. Therefore, caution should be exercised when directly comparing our results on AA taste responses to those of others who used electrophysiological recordings. ^{59,82,84} Finally, previous work has identified a role for IR co-receptors in egg laying on acids and polyamines, ^{85,86} and while we would have liked to further test the role of IR25a and IR76b in oviposition, the broad functions of these receptors across multiple GRN types makes interpretation of their phenotypes difficult in the absence of cell-type-specific manipulation.

STAR*METHODS

Detailed methods are provided in the online version of this paper and include the following:

- KEY RESOURCES TABLE
- RESOURCE AVAILABILITY
 - Lead contact
 - Materials availability
 - Data and code availability
- EXPERIMENTAL MODEL AND STUDY PARTICIPANT DETAILS
 - Flies
- METHOD DETAILS
 - Chemicals
 - o Immunohistochemistry
 - Feeding assays
 - o Egg-laying assays
 - $\, \circ \, \, \, \text{Calcium imaging} \, \,$
 - $\ \, \circ \ \, \text{Connectomics analysis}$
 - Fly Cell Atlas analysis
- QUANTIFICATION AND STATISTICAL ANALYSIS

SUPPLEMENTAL INFORMATION

Supplemental information can be found online at https://doi.org/10.1016/j.celrep.2024.114625.

ACKNOWLEDGMENTS

We thank the Bloomington Stock Center and the Vienna Drosophila Resource Center for fly stocks and Dr. Pierre Junca for generating the split-Gal4 driver line. We thank the Princeton FlyWire team and members of the Murthy and Seung labs, as well as members of the Allen Institute for Brain Science, for development and maintenance of FlyWire (supported by BRAIN Initiative grants MH117815 and NS126935 to Murthy and Seung). We also acknowledge members of the Princeton FlyWire team and the FlyWire consortium for neuron proofreading and annotation. Specific acknowledgments for the connectome neurons in this study are located in Tables S1–S3. This work was funded by the Canadian Institutes of Health Research grants FDN-148424 and PJT-180583 (M.D.G.), the National Science Foundation award 2332375 (M.S.), and the University of Vermont OVPR Express grant and lab startup funds (M.S.).

AUTHOR CONTRIBUTIONS

Conceptualization, M.D.G. and M.S.; methodology, J.G., J.L., M.D.G., and M.S.; investigation, J.G., J.L., S.A.T.M., V.L., K.A., G.D., M.J., S.S., L.K., and M.S.; writing – original draft, J.G. and M.S.; writing – review & editing, J.G.,

Article



J.L., S.A.T.M., K.A., G.D., M.J., M.D.G., and M.S.; visualization, J.G., J.L., and M.S.; resources, M.D.G. and M.S.; supervision, M.D.G. and M.S.; funding acquisition, M.D.G. and M.S.

DECLARATION OF INTERESTS

The authors declare no competing interests.

Received: February 2, 2024 Revised: June 1, 2024 Accepted: July 30, 2024

REFERENCES

- Yohe, L.R., and Brand, P. (2018). Evolutionary ecology of chemosensation and its role in sensory drive. Curr. Zool. 64, 525–533. https://doi.org/10. 1093/cz/zoy048.
- Thoma, V., Kobayashi, K., and Tanimoto, H. (2017). The Role of the Gustatory System in the Coordination of Feeding. eneuro 4, e0324-17. https://doi.org/10.1523/eneuro.0324-17.2017.
- Cury, K.M., Prud'homme, B., and Gompel, N. (2019). A short guide to insect oviposition: when, where and how to lay an egg. J. Neurogenet. 33, 75–89. https://doi.org/10.1080/01677063.2019.1586898.
- Dorkenwald, S., Matsliah, A., Sterling, A.R., Schlegel, P., Yu, S.C., McKellar, C.E., Lin, A., Costa, M., Eichler, K., Yin, Y., et al. (2023). Neuronal wiring diagram of an adult brain. Preprint at bioRxiv. https://doi.org/10.1101/2023.06.27.546656.
- Dorkenwald, S., McKellar, C.E., Macrina, T., Kemnitz, N., Lee, K., Lu, R., Wu, J., Popovych, S., Mitchell, E., Nehoran, B., et al. (2022). FlyWire: online community for whole-brain connectomics. Nat. Methods 19, 119–128. https://doi.org/10.1038/s41592-021-01330-0.
- Zheng, Z., Lauritzen, J.S., Perlman, E., Robinson, C.G., Nichols, M., Milkie, D., Torrens, O., Price, J., Fisher, C.B., Sharifi, N., et al. (2018). A Complete Electron Microscopy Volume of the Brain of Adult Drosophila melanogaster. Cell 174, 730–743.e22. https://doi.org/10.1016/j.cell.2018. 06.019.
- Devineni, A.V., and Scaplen, K.M. (2021). Neural Circuits Underlying Behavioral Flexibility: Insights From Drosophila. Front. Behav. Neurosci. 15, 821680. https://doi.org/10.3389/fnbeh.2021.821680.
- González Segarra, A.J., Pontes, G., Jourjine, N., Del Toro, A., and Scott, K. (2023). Hunger- and thirst-sensing neurons modulate a neuroendocrine network to coordinate sugar and water ingestion. Elife 12, RP88143. https://doi.org/10.7554/eLife.88143.
- Hulse, B.K., Haberkern, H., Franconville, R., Turner-Evans, D., Takemura, S.Y., Wolff, T., Noorman, M., Dreher, M., Dan, C., Parekh, R., et al. (2021). A connectome of the Drosophila central complex reveals network motifs suitable for flexible navigation and context-dependent action selection. Elife 10, e66039. https://doi.org/10.7554/eLife.66039.
- Cheriyamkunnel, S.J., Rose, S., Jacob, P.F., Blackburn, L.A., Glasgow, S., Moorse, J., Winstanley, M., Moynihan, P.J., Waddell, S., and Rezaval, C. (2021). A neuronal mechanism controlling the choice between feeding and sexual behaviors in Drosophila. Curr. Biol. 31, 4231–4245.e4. https://doi.org/10.1016/j.cub.2021.07.029.
- Taisz, I., Donà, E., Münch, D., Bailey, S.N., Morris, B.J., Meechan, K.I., Stevens, K.M., Varela-Martínez, I., Gkantia, M., Schlegel, P., et al. (2023). Generating parallel representations of position and identity in the olfactory system. Cell 186, 2556–2573.e22. https://doi.org/10.1016/j. cell.2023.04.038.
- Koganezawa, M., Kimura, K.-i., and Yamamoto, D. (2016). The neural circuitry that functions as a switch for courtship versus aggression in Drosophila males. Curr. Biol. 26, 1395–1403.

- Stocker, R.F. (1994). The organization of the chemosensory system in Drosophila melanogaster: a review. Cell Tissue Res. 275, 3–26. https://doi.org/10.1007/bf00305372.
- Scott, K. (2018). Gustatory Processing in Drosophila melanogaster. Annu. Rev. Entomol. 63, 15–30. https://doi.org/10.1146/annurev-ento-020117-043331
- Montell, C. (2021). Drosophila sensory receptors-a set of molecular Swiss Army Knives. Genetics 217, 1–34. https://doi.org/10.1093/genetics/ivaa011.
- Marella, S., Fischler, W., Kong, P., Asgarian, S., Rueckert, E., and Scott, K. (2006). Imaging taste responses in the fly brain reveals a functional map of taste category and behavior. Neuron 49, 285–295. https://doi.org/10.1016/j.neuron.2005.11.037.
- Chen, H.L., Motevalli, D., Stern, U., and Yang, C.H. (2022). A functional division of Drosophila sweet taste neurons that is value-based and task-specific. Proc. Natl. Acad. Sci. USA 119, e2110158119. https://doi.org/10.1073/pnas.2110158119.
- Joseph, R.M., and Heberlein, U. (2012). Tissue-specific activation of a single gustatory receptor produces opposing behavioral responses in Drosophila. Genetics 192, 521–532. https://doi.org/10.1534/genetics. 112 142455
- Lihoreau, M., Poissonnier, L.-A., Isabel, G., and Dussutour, A. (2016). Drosophila females trade off good nutrition with high-quality oviposition sites when choosing foods. J. Exp. Biol. 219, 2514–2524. https://doi. org/10.1242/jeb.142257.
- Schwartz, N.U., Zhong, L., Bellemer, A., and Tracey, W.D. (2012). Egg laying decisions in Drosophila are consistent with foraging costs of larval progeny. PLoS One 7, e37910. https://doi.org/10.1371/journal.pone. 0037910.
- Yang, C.H., Belawat, P., Hafen, E., Jan, L.Y., and Jan, Y.N. (2008).
 Drosophila egg-laying site selection as a system to study simple decision-making processes. Science 319, 1679–1683. https://doi.org/10.1126/science.1151842.
- Cury, K.M., and Axel, R. (2023). Flexible neural control of transition points within the egg-laying behavioral sequence in Drosophila. Nat. Neurosci. 26, 1054–1067. https://doi.org/10.1038/s41593-023-01332-5.
- Bräcker, L.B., Schmid, C.A., Bolini, V.A., Holz, C.A., Prud'homme, B., Sirota, A., and Gompel, N. (2019). Quantitative and Discrete Evolutionary Changes in the Egg-Laying Behavior of Single Drosophila Females. Front. Behav. Neurosci. 13, 118. https://doi.org/10.3389/fnbeh.2019.00118.
- Joseph, R.M., Devineni, A.V., King, I.F.G., and Heberlein, U. (2009). Oviposition preference for and positional avoidance of acetic acid provide a model for competing behavioral drives in Drosophila. Proc. Natl. Acad. Sci. USA 106, 11352–11357. https://doi.org/10.1073/pnas.0901419106.
- Jaeger, A.H., Stanley, M., Weiss, Z.F., Musso, P.Y., Chan, R.C., Zhang, H., Feldman-Kiss, D., and Gordon, M.D. (2018). A complex peripheral code for salt taste in Drosophila. Elife 7, e37167. https://doi.org/10.7554/eLife. 37167
- Koh, T.W., He, Z., Gorur-Shandilya, S., Menuz, K., Larter, N.K., Stewart, S., and Carlson, J.R. (2014). The Drosophila IR20a clade of ionotropic receptors are candidate taste and pheromone receptors. Neuron 83, 850–865. https://doi.org/10.1016/j.neuron.2014.07.012.
- Croset, V., Schleyer, M., Arguello, J.R., Gerber, B., and Benton, R. (2016).
 A molecular and neuronal basis for amino acid sensing in the Drosophila larva. Sci. Rep. 6, 34871. https://doi.org/10.1038/srep34871.
- Sánchez-Alcañiz, J.A., Silbering, A.F., Croset, V., Zappia, G., Sivasubramaniam, A.K., Abuin, L., Sahai, S.Y., Münch, D., Steck, K., Auer, T.O., et al. (2018). An expression atlas of variant ionotropic glutamate receptors identifies a molecular basis of carbonation sensing. Nat. Commun. 9, 4252. https://doi.org/10.1038/s41467-018-06453-1.
- Venkatasubramanian, L., and Mann, R.S. (2019). The development and assembly of the Drosophila adult ventral nerve cord. Curr. Opin. Neurobiol. 56, 135–143. https://doi.org/10.1016/j.conb.2019.01.013.





- McDowell, S.A.T., Stanley, M., and Gordon, M.D. (2022). A molecular mechanism for high salt taste in Drosophila. Curr. Biol. 32, 3070– 3081.e5. https://doi.org/10.1016/j.cub.2022.06.012.
- Li, H., Janssens, J., De Waegeneer, M., Kolluru, S.S., Davie, K., Gardeux, V., Saelens, W., David, F.P.A., Brbić, M., Spanier, K., et al. (2022). Fly Cell Atlas: A single-nucleus transcriptomic atlas of the adult fruit fly. Science 375, eabk2432. https://doi.org/10.1126/science.abk2432.
- Bontonou, G., Saint-Leandre, B., Kafle, T., Baticle, T., Hassan, A., Sán-chez-Alcañiz, J.A., and Arguello, J.R. (2024). Evolution of chemosensory tissues and cells across ecologically diverse Drosophilids. Nat. Commun. 15, 1047. https://doi.org/10.1038/s41467-023-44558-4.
- Shiraiwa, T., and Carlson, J.R. (2007). Proboscis extension response (PER) assay in Drosophila. J. Vis. Exp. 193, 193. https://doi.org/10. 3791/193.
- Gordon, M.D., and Scott, K. (2009). Motor control in a Drosophila taste circuit. Neuron 61, 373–384. https://doi.org/10.1016/j.neuron.2008.12.033.
- Shiu, P.K., Sterne, G.R., Engert, S., Dickson, B.J., and Scott, K. (2022).
 Taste quality and hunger interactions in a feeding sensorimotor circuit.
 Elife 11, e79887. https://doi.org/10.7554/eLife.79887.
- Deere, J.U., and Devineni, A.V. (2022). Taste cues elicit prolonged modulation of feeding behavior in Drosophila. iScience 25, 105159. https://doi.org/10.1016/j.isci.2022.105159.
- 37. Shiu, P.K., Sterne, G.R., Spiller, N., Franconville, R., Sandoval, A., Zhou, J., Simha, N., Kang, C.H., Yu, S., Kim, J.S., et al. (2023). A leaky integrate-and-fire computational model based on the connectome of the entire adult Drosophila brain reveals insights into sensorimotor processing. Preprint at bioRxiv. https://doi.org/10.1101/2023.05.02.539144.
- Musso, P.Y., Junca, P., Jelen, M., Feldman-Kiss, D., Zhang, H., Chan, R.C., and Gordon, M.D. (2019). Closed-loop optogenetic activation of peripheral or central neurons modulates feeding in freely moving Drosophila. Elife 8, e45636. https://doi.org/10.7554/eLife.45636.
- May, C.E., Vaziri, A., Lin, Y.Q., Grushko, O., Khabiri, M., Wang, Q.P., Holme, K.J., Pletcher, S.D., Freddolino, P.L., Neely, G.G., and Dus, M. (2019). High Dietary Sugar Reshapes Sweet Taste to Promote Feeding Behavior in Drosophila melanogaster. Cell Rep. 27, 1675–1685.e7. https://doi.org/10.1016/j.celrep.2019.04.027.
- Ro, J., Harvanek, Z.M., and Pletcher, S.D. (2014). FLIC: high-throughput, continuous analysis of feeding behaviors in Drosophila. PLoS One 9, e101107
- Itskov, P.M., Moreira, J.M., Vinnik, E., Lopes, G., Safarik, S., Dickinson, M.H., and Ribeiro, C. (2014). Automated monitoring and quantitative analysis of feeding behaviour in Drosophila. Nat. Commun. 5, 4560. https://doi. org/10.1038/ncomms5560.
- Caterina, M.J., Schumacher, M.A., Tominaga, M., Rosen, T.A., Levine, J.D., and Julius, D. (1997). The capsaicin receptor: a heat-activated ion channel in the pain pathway. Nature 389, 816–824. https://doi.org/10. 1038/39807.
- Eckstein, N., Bates, A.S., Champion, A., Du, M., Yin, Y., Schlegel, P., Lu, A.K.Y., Rymer, T., Finley-May, S., Paterson, T., et al. (2024). Neurotransmitter classification from electron microscopy images at synaptic sites in Drosophila melanogaster. Cell 187, 2574–2594.e2523. https://doi.org/ 10.1016/j.cell.2024.03.016.
- Schlegel, P., Yin, Y., Bates, A.S., Dorkenwald, S., Eichler, K., Brooks, P., Han, D.S., Gkantia, M., Dos Santos, M., Munnelly, E.J., et al. (2023). Whole-brain annotation and multi-connectome cell typing quantifies circuit stereotypy in Drosophila. Preprint at bioRxiv. https://doi.org/10. 1101/2023.06.27.546055.
- Sterne, G.R., Otsuna, H., Dickson, B.J., and Scott, K. (2021). Classification and genetic targeting of cell types in the primary taste and premotor center of the adult Drosophila brain. Elife 10, e71679. https://doi.org/10.7554/eLife.71679.
- Deere, J.U., Sarkissian, A.A., Yang, M., Uttley, H.A., Martinez Santana, N., Nguyen, L., Ravi, K., and Devineni, A.V. (2023). Selective integration of

- diverse taste inputs within a single taste modality. Elife 12, e84856. https://doi.org/10.7554/eLife.84856.
- Jacobs, R.V., Wang, C.X., Lozada-Perdomo, F.V., Nguyen, L., Deere, J.U., Uttley, H.A., and Devineni, A.V. (2023). Overlap and divergence of neural circuits mediating distinct behavioral responses to sugar. Preprint at bio-Rxiv. https://doi.org/10.1101/2023.10.01.560401.
- Engert, S., Sterne, G.R., Bock, D.D., and Scott, K. (2022). Drosophila gustatory projections are segregated by taste modality and connectivity. Elife 11, e78110. https://doi.org/10.7554/eLife.78110.
- Costa, M., Manton, J.D., Ostrovsky, A.D., Prohaska, S., and Jefferis, G.S.X.E. (2016). NBLAST: Rapid, Sensitive Comparison of Neuronal Structure and Construction of Neuron Family Databases. Neuron 91, 293–311. https://doi.org/10.1016/j.neuron.2016.06.012.
- Wang, F., Wang, K., Forknall, N., Patrick, C., Yang, T., Parekh, R., Bock, D., and Dickson, B.J. (2020). Neural circuitry linking mating and egg laying in Drosophila females. Nature 579, 101–105. https://doi.org/10.1038/ s41586-020-2055-9.
- Tirian, L., and Dickson, B.J. (2017). The VT GAL4, LexA, and split-GAL4 driver line collections for targeted expression in the Drosophila nervous system. Preprint at bioRxiv. https://doi.org/10.1101/198648.
- Dionne, H., Hibbard, K.L., Cavallaro, A., Kao, J.-C., and Rubin, G.M. (2017). Genetic reagents for making split-GAL4 lines in Drosophila. Preprint at bioRxiv. https://doi.org/10.1101/197509.
- Yao, Z., Macara, A.M., Lelito, K.R., Minosyan, T.Y., and Shafer, O.T. (2012). Analysis of functional neuronal connectivity in the Drosophila brain.
 J. Neurophysiol. 108, 684–696. https://doi.org/10.1152/jn.00110.2012.
- Valera, S., Hussy, N., Evans, R.J., Adami, N., North, R.A., Surprenant, A., and Buell, G. (1994). A new class of ligand-gated ion channel defined by P2x receptor for extracellular ATP. Nature 371, 516–519. https://doi.org/ 10.1038/371516a0.
- Benton, R., Vannice, K.S., Gomez-Diaz, C., and Vosshall, L.B. (2009).
 Variant ionotropic glutamate receptors as chemosensory receptors in Drosophila. Cell 136, 149–162. https://doi.org/10.1016/j.cell.2008.12.001.
- Croset, V., Rytz, R., Cummins, S.F., Budd, A., Brawand, D., Kaessmann, H., Gibson, T.J., and Benton, R. (2010). Ancient protostome origin of chemosensory ionotropic glutamate receptors and the evolution of insect taste and olfaction. PLoS Genet. 6, e1001064. https://doi.org/10.1371/ journal.pgen.1001064.
- Rytz, R., Croset, V., and Benton, R. (2013). Ionotropic receptors (IRs): chemosensory ionotropic glutamate receptors in Drosophila and beyond. Insect Biochem. Mol. Biol. 43, 888–897. https://doi.org/10.1016/j.ibmb. 2013.02.007
- Dweck, H.K.M., Talross, G.J.S., Luo, Y., Ebrahim, S.A.M., and Carlson, J.R. (2022). Ir56b is an atypical ionotropic receptor that underlies appetitive salt response in Drosophila. Curr. Biol. 32, 1776–1787.e4. https://doi.org/10.1016/j.cub.2022.02.063.
- Aryal, B., Dhakal, S., Shrestha, B., and Lee, Y. (2022). Molecular and neuronal mechanisms for amino acid taste perception in the Drosophila labellum. Curr. Biol. 32, 1376–1386.e4. https://doi.org/10.1016/j.cub. 2022.01.060.
- Govorunova, E.G., Sineshchekov, O.A., Janz, R., Liu, X., and Spudich, J.L. (2015). Natural light-gated anion channels: A family of microbial rhodopsins for advanced optogenetics. Science 349, 647–650.
- Kliewer, W.M. (1968). Changes in the Concentration of Free Amino Acids in Grape Berries During Maturation. Am. J. Enol. Vitic. 19, 166–174. https://doi.org/10.5344/ajev.1968.19.3.166.
- Kersh, D.M.E., Hammad, G., Donia, M.S., and Farag, M.A. (2023). A Comprehensive Review on Grape Juice Beverage in Context to Its Processing and Composition with Future Perspectives to Maximize Its Value. Food Bioprocess Technol. 16, 1–23. https://doi.org/10.1007/s11947-022-02858-5.

Article



- Yamamoto, D., and Koganezawa, M. (2013). Genes and circuits of courtship behaviour in Drosophila males. Nat. Rev. Neurosci. 14, 681–692. https://doi.org/10.1038/nrn3567.
- 64. Lacaille, F., Hiroi, M., Twele, R., Inoshita, T., Umemoto, D., Manière, G., Marion-Poll, F., Ozaki, M., Francke, W., Cobb, M., et al. (2007). An Inhibitory Sex Pheromone Tastes Bitter for Drosophila Males. PLoS One 2, e661. https://doi.org/10.1371/journal.pone.0000661.
- Nelson, G., Chandrashekar, J., Hoon, M.A., Feng, L., Zhao, G., Ryba, N.J.P., and Zuker, C.S. (2002). An amino-acid taste receptor. Nature 416, 199–202. https://doi.org/10.1038/nature726.
- Kawai, M., Sekine-Hayakawa, Y., Okiyama, A., and Ninomiya, Y. (2012).
 Gustatory sensation of I- and d-amino acids in humans. Amino Acids 43, 2349–2358. https://doi.org/10.1007/s00726-012-1315-x.
- Kohl, S., Behrens, M., Dunkel, A., Hofmann, T., and Meyerhof, W. (2013).
 Amino Acids and Peptides Activate at Least Five Members of the Human Bitter Taste Receptor Family. J. Agric. Food Chem. 61, 53–60. https://doi. org/10.1021/if303146h.
- Bassoli, A., Borgonovo, G., Caremoli, F., and Mancuso, G. (2014). The taste of D-and L-amino acids: In vitro binding assays with cloned human bitter (TAS2Rs) and sweet (TAS1R2/TAS1R3) receptors. Food Chem. 150, 27–33.
- Chaudhari, N., Pereira, E., and Roper, S.D. (2009). Taste receptors for umami: the case for multiple receptors. Am. J. Clin. Nutr. 90, 738S– 742S. https://doi.org/10.3945/ajcn.2009.27462H.
- Diepeveen, J., Moerdijk-Poortvliet, T.C., and van der Leij, F.R. (2022). Molecular insights into human taste perception and umami tastants: A review. J. Food Sci. 87. 1449–1465.
- Pal Choudhuri, S., Delay, R.J., and Delay, E.R. (2015). L-amino acids elicit diverse response patterns in taste sensory cells: a role for multiple receptors. PLoS One 10, e0130088.
- Bachmanov, A.A., Bosak, N.P., Glendinning, J.I., Inoue, M., Li, X., Manita, S., McCaughey, S.A., Murata, Y., Reed, D.R., Tordoff, M.G., and Beauchamp, G.K. (2016). Genetics of Amino Acid Taste and Appetite. Adv. Nutr. 7, 806s–822S. https://doi.org/10.3945/an.115.011270.
- Steck, K., Walker, S.J., Itskov, P.M., Baltazar, C., Moreira, J.M., and Ribeiro, C. (2018). Internal amino acid state modulates yeast taste neurons to support protein homeostasis in Drosophila. Elife 7, e31625. https://doi.org/10.7554/eLife.31625.
- Li, X., Staszewski, L., Xu, H., Durick, K., Zoller, M., and Adler, E. (2002). Human receptors for sweet and umami taste. Proc. Natl. Acad. Sci. USA 99, 4692–4696.
- Bowman, E., and Tatar, M. (2016). Reproduction regulates Drosophila nutrient intake through independent effects of egg production and sex peptide: Implications for aging. Nutr. Healthy Aging 4, 55–61. https://doi. org/10.3233/NHA-1613.
- Ganguly, A., Pang, L., Duong, V.K., Lee, A., Schoniger, H., Varady, E., and Dahanukar, A. (2017). A Molecular and Cellular Context-Dependent Role for Ir76b in Detection of Amino Acid Taste. Cell Rep. 18, 737–750. https://doi.org/10.1016/j.celrep.2016.12.071.
- 77. Vargas, M.A., Luo, N., Yamaguchi, A., and Kapahi, P. (2010). A role for S6 kinase and serotonin in postmating dietary switch and balance of nutrients

- in D. melanogaster. Curr. Biol. 20, 1006–1011. https://doi.org/10.1016/j.cub.2010.04.009.
- Ribeiro, C., and Dickson, B.J. (2010). Sex peptide receptor and neuronal TOR/S6K signaling modulate nutrient balancing in Drosophila. Curr. Biol. 20, 1000–1005. https://doi.org/10.1016/j.cub.2010.03.061.
- Becher, P.G., Flick, G., Rozpędowska, E., Schmidt, A., Hagman, A., Lebreton, S., Larsson, M.C., Hansson, B.S., Piškur, J., Witzgall, P., and Bengtsson, M. (2012). Yeast, not fruit volatiles mediate Drosophila melanogaster attraction, oviposition and development. Funct. Ecol. 26, 822–828. https://doi.org/10.1111/j.1365-2435.2012.02006.x.
- Loï, C., and Cynober, L. (2022). Glutamate: A Safe Nutrient, Not Just a Simple Additive. Ann. Nutr. Metab. 78, 133–146. https://doi.org/10.1159/ 000522482
- Campbell, A. (2005). In Encyclopedia of Toxicology, Second Edition, P. Wexler, ed. (Elsevier), pp. 150–152.
- Ganguly, A., Dey, M., Scott, C., Duong, V.-K., and Arun Dahanukar, A. (2021). Dietary Macronutrient Imbalances Lead to Compensatory Changes in Peripheral Taste via Independent Signaling Pathways.
 J. Neurosci. 41, 10222–10246. https://doi.org/10.1523/JNEUROSCI. 2154-20.2021.
- Ohkura, M., Sasaki, T., Sadakari, J., Gengyo-Ando, K., Kagawa-Nagamura, Y., Kobayashi, C., Ikegaya, Y., and Nakai, J. (2012). Genetically encoded green fluorescent Ca2+ indicators with improved detectability for neuronal Ca2+ signals. PLoS One 7, e51286. https://doi.org/10.1371/journal.pone.0051286.
- Dahanukar, A., Lei, Y.-T., Kwon, J.Y., and Carlson, J.R. (2007). Two Gr Genes Underlie Sugar Reception in Drosophila. Neuron 56, 503–516. https://doi.org/10.1016/j.neuron.2007.10.024.
- Chen, Y., and Amrein, H. (2017). Ionotropic Receptors Mediate Drosophila Oviposition Preference through Sour Gustatory Receptor Neurons. Curr. Biol. 27, 2741–2750.e4. https://doi.org/10.1016/j.cub.2017.08.003.
- Hussain, A., Zhang, M., Üçpunar, H.K., Svensson, T., Quillery, E., Gompel, N., Ignell, R., and Grunwald Kadow, I.C. (2016). Ionotropic Chemosensory Receptors Mediate the Taste and Smell of Polyamines. PLoS Biol. 14, e1002454. https://doi.org/10.1371/journal.pbio.1002454.
- Yavuz, A., Jagge, C., Slone, J., and Amrein, H. (2014). A genetic tool kit for cellular and behavioral analyses of insect sugar receptors. Fly 8, 189–196. https://doi.org/10.1080/19336934.2015.1050569.
- 88. Wang, Z., Singhvi, A., Kong, P., and Scott, K. (2004). Taste representations in the Drosophila brain. Cell *1117*, 981–991.
- 89. Zhang, Y.V., Ni, J., and Montell, C. (2013). The molecular basis for attractive salt-taste coding in Drosophila. Science *340*, 1334–1338.
- Lai, S.L., and Lee, T. (2006). Genetic mosaic with dual binary transcriptional systems in Drosophila. Nat. Neurosci. 9, 703–709. https://doi.org/10.1038/nn1681.
- Schneider, C.A., Rasband, W.S., and Eliceiri, K.W. (2012). NIH Image to ImageJ: 25 years of image analysis. Nat. Methods 9, 671–675. https://doi.org/10.1038/nmeth.2089.
- Stanley, M., Ghosh, B., Weiss, Z.F., Christiaanse, J., and Gordon, M.D. (2021). Mechanisms of lactic acid gustatory attraction in Drosophila. Curr. Biol. 31, 3525–3537.e6. https://doi.org/10.1016/j.cub.2021.06.005.





STAR***METHODS**

KEY RESOURCES TABLE

REAGENT or RESOURCE	SOURCE	IDENTIFIER
Antibodies		
Goat anti- mouse 546	Invitrogen	Cat# A11030; RRID: AB_2534089
Goat anti- rabbit 647	Invitrogen	Cat# A21245; RRID: AB_2535813
Goat anti-chicken 488	AbCam	Cat# 150169; RRID: AB_2636803
Chicken anti-GFP	AbCam	Cat# 13970; RRID: AB_300798
Rabbit anti-RFP	Rockland	Cat# A11122
mouse anti-brp	DSHB	Cat# nc82; RRID: AB_2314866
Chemicals, peptides, and recombinant	t proteins	
Ethanol	Pharmco	111000200
Sucrose	Sigma-Aldrich	S7903
Capsaicin	Sigma-Aldrich	M2028
NaCl	Sigma-Aldrich	S7653
KCI	Sigma-Aldrich	P9541
L-Na ⁺ Glutamate	Sigma-Aldrich	49621
L-K ⁺ Glutamate	Sigma-Aldrich	G1501
L-Glutamic acid	Sigma-Aldrich	G1251
L-K ⁺ Aspartate	Sigma-Aldrich	11230
L-Lysine (HCI)	Sigma-Aldrich	L5626
L-Leucine	Sigma-Aldrich	L8000
L-Phenylalanine	Sigma-Aldrich	P5482
L-Valine	Sigma-Aldrich	V0500
L-Proline	Sigma-Aldrich	P0380
Serine	Sigma-Aldrich	84959
Glycine	Sigma-Aldrich	50046
Hexanoic acid	Sigma-Aldrich	H12137
Sodium bicarbonate	Sigma-Aldrich	S6014
Tryptone	Fisher Bioreagents	BP1421-2
Yeast extract	Fisher Bioreagents	BP1422-500
Active Dry Yeast	Genesee Scientific	62–103
Agar	Sigma-Aldrich	A1296
DL-Lactic acid	Sigma-Aldrich	69785
All-trans-Retinal	Sigma-Aldrich	R2500
Grape juice- concord grape	Welch's	N/A
7,11-heptacosadiene (7,11-HC)	Caymen chemical company	10012567
7,11-nonacosadiene (7,11-NC)	Caymen chemical company	9000314
7-tricosene (7 T)	Caymen chemical company	9000313
Cis-vaccenyl acetate (c-VA)	Caymen chemical company	10010101
Erioglaucine, FD&C Blue #1	Sigma-Aldrich	861146
Amaranth (red)	Sigma-Aldrich	A1016
2Na-ATP	Sigma-Aldrich	A1852

(Continued on next page)

Cell Reports Article



Continued		
REAGENT or RESOURCE	SOURCE	IDENTIFIER
Deposited data		
FLIC analysis code	This study, Pletcher Lab	Github Code: http://github.com/MStanleyLab/FLIC_code
Mendeley dataset	This study	Mendeley Data: https://doi.org/ 10.17632/d8bvxb3yfm.1
Experimental models: Organisms/strains		
D.melanogaster: w1118	Wellgenetics (isogenic control for <i>IR94e</i> knock-in)	RRID: BDSC_3605
D.melanogaster: IR94e-Gal4	Koh et al. ²⁶	RRID: BDSC_60725 Flybase: FBtp0095585
D.melanogaster: IR94e-Gal4	Croset et al. ²⁷	RRID: BDSC_81246 Flybase: FBti0202323
D.melanogaster: Ir94e-Gal4(VT)	Tirian & Dickson ⁵¹	VDRC: v207582
D.melanogaster: IR94eLexA	McDowell et al.30	Flybase: FBal0376356
D.melanogaster: Gr64f-Gal4	Dahanukar et al. ⁸⁴	Flybase: FBtp0057275
D.melanogaster: Gr64fLexA	Yavuz et al. ⁸⁷	RRID: BDSC_93445 Flybase: FBal0304291
D.melanogaster: Gr66a-Gal4	Wang et al. ⁸⁸	RRID: BDSC_28801 Flybase: FBtp0014660
D.melanogaster: IR7c ^{GAL4}	McDowell et al.30	N/A
D.melanogaster: IR25a ¹	Benton et al. ⁵⁵	RRID: BDSC_41736 Flybase: FBst0041736
D.melanogaster: IR25a ²	Benton et al. ⁵⁵	RRID: BDSC_41737 Flybase: FBst0041737
D.melanogaster: IR76b ¹	Zhang et al. ⁸⁹	RRID: BDSC_51309 Flybase: FBst0051309
D.melanogaster: IR76b ²	Zhang et al. ⁸⁹	RRID: BDSC_51310 Flybase: FBst0051310
D.melanogaster: LexAop-csChrimson	Bloomington Drosophila Stock Center	RRID: BDSC_55138
D.melanogaster: LexAop-P2X2	Yao et al. ⁵³	RRID: BDSC_76030
D.melanogaster: LexAop-GCaMP6f	Bloomington Drosophila Stock Center	RRID: BDSC_44277
D.melanogaster: UAS-GCaMP6f	Bloomington Drosophila Stock Center	RRID: BDSC_52869
D.melanogaster: UAS-jGCaMP7f	Bloomington Drosophila Stock Center	RRID: BDSC_80906
D.melanogaster: UAS-jGCaMP7f	Bloomington Drosophila Stock Center	RRID: BDSC_79031
D.melanogaster: UAS-csChrimson	Bloomington Drosophila Stock Center	RRID: BDSC_55135
D.melanogaster: LexAop-rCD2::GFP	Lai and Lee ⁹⁰	RRID: BDSC_66687 Flybase: FBti0186090
D.melanogaster: UAS-tdTomato	Bloomington Drosophila Stock Center	RRID: BDSC_36327
D.melanogaster: UAS-VR1E600K	Marella et al. 16	N/A
D.melanogaster: UAS-IR94e	This study	N/A
D.melanogaster: VT019729-p65.AD	Bloomington Drosophila Stock Center	RRID: BDSC_73020 FBsf0000446785
D.melanogaster: VT008484-GAL4.DBD	Bloomington Drosophila Stock Center	RRID: BDSC_74557 FBsf0000447968
Software and algorithms		
ImageJ	Schneider et al. ⁹¹	RRID: SCR_002285, SCR_003070 https://imagej.nih.gov/ij
Slidebook 2023	3i (Intelligent Imaging Innovations)	RRID: SCR_014300 https://www.intelligent-imaging.com/slidebool
STROBE	Musso et al. ³⁸	http://github.com/rcwchan/ STROBE_software
		=

(Continued on next page)





Continued		
REAGENT or RESOURCE	SOURCE	IDENTIFIER
R Studio (4.3.2)	RStudio Team	RRID: SCR_000432 https://www.rstudio.com/
Navis (1.6.0)	Costa et al. ⁴⁹	https://navis.readthedocs.io/en/latest/ source/tutorials/nblast.html
Python (5.18.0)	Plotly Graphing Libraries	RRID: SCR_008394 https://plotly.com/python/
Illustrator	Adobe	RRID: SCR_010279 https://www.adobe.com
Prism 10	Graphpad	RRID: SCR_002798 https://www.graphpad.com/ scientificsoftware/prism/
BioRender	BioRender	RRID: SCR_018361 https://www.biorender.com

RESOURCE AVAILABILITY

Lead contact

Additional information and requests for resources and reagents should be directed to and will be fulfilled by the lead contact, Molly Stanley (molly.stanley@uvm.edu).

Materials availability

New fly lines generated by this project will be shared upon request.

Data and code availability

- All raw data presented in the figures of this manuscript have been published on a Mendeley data online repository (link in the key resources table).
- All custom code used for the FLIC data analysis has been deposited on GitHub (link in the key resources table).
- Any additional information required to reanalyze the data reported in this paper is available from the lead contact upon request.

EXPERIMENTAL MODEL AND STUDY PARTICIPANT DETAILS

Flies

Experimental flies were kept at 25°C in 60% relative humidity prior to the experiment and on regular cornmeal food unless indicated otherwise. Mated females were used except where males are indicated. All experimental flies were between 2 and 10 days old. Each genotype is shown near the relevant datasets in each figure and detailed information for each previously generated *Drosophila* line used in these experiments is located in the key resources table. The *UAS-IR94e* transgenic line was created by synthesizing the coding sequence of IR94e and subcloning into the PUAST-attB vector before injection and integration into the attP40 site of *w1118* embryos. Synthesis was performed by Bio Basic (Ontario, Canada). Subcloning and injections were performed by GenetiVision (Texas, USA).

METHOD DETAILS

Chemicals

A full list of chemicals with source information can be found in the key resources table. Sucrose, NaCl, KCl, K $^+$ glutamate, Na $^+$ glutamate, K $^+$ aspartate, valine, lysine, proline, leucine, phenylalanine, glycine, serine, lactic acid, NaHCO $_3$, and Na-ATP were dissolved in water at the specified concentrations. Glutamic acid was dissolved in water at a maximum solubility of 50 mM. Tryptone and yeast extract were freshly made up in water at the indicated w/v% solutions. Grape juice was used at a final concentration of 25% v/v. Capsaicin was made up in a 100 mM stock in 70% EtOH and diluted to a final concentration of 100 μ M capsaicin in water, vehicle was 0.07% EtOH. Pheromones in the form of 7,11 heptacosadiene (7,11-HC), 7,11-nonacosadiene (7,11-NC), and 7-tricosene (7 T) were diluted in water to 0.0001 mg/ul. Cis-vaccenyl acetate (c-VA) was diluted to a stock solution of 0.01 mg/ μ L in EtOH, and then diluted in water. Hexanoic acid at 1% was made up in water. Pheromones and most other stocks were kept at 4°C. All-trans-retinal (ATR) was made up in 100% EtOH, kept at -20° C, and diluted to a final concentration of 1 mM with EtOH of the same dilution given as a vehicle.

Cell ReportsArticle



Immunohistochemistry

Immunofluorescence on labella, brains, VNC, and front tarsi was carried out as described previously. ^{25,30} Briefly, labella and tarsi were dissected and then fixed in 4% paraformaldehyde in PBS +0.2% Triton (PBST) for 30 min before washing in 0.2% PBST, whereas full flies were fixed for 45 min in 4% paraformaldehyde in 0.1% Triton before brain and VNC dissections. Tissues were blocked in 5% normal goat serum (NGS) before adding primary antibodies (chick anti-GFP at 1:1000, rabbit anti-RFP at 1:200, anti-brp 1:50) overnight. After washing in PBST, secondary antibodies (goat anti-chicken Alexa 488, goat anti-rabbit Alexa 647, goat anti-mouse Alexa 546, all 1:200) were incubated overnight. After washing in PBST, samples were placed on slides in SlowFade gold with #1 coverslips as spacers. Images were acquired using a Leica SP5 II Confocal microscope with 25× water immersion objective or 63× oil immersion objective, or on a 3i Spinning disc Confocal station (Zeiss upright microscope, 2 K × 2 K 40 fps sCMOS camera, CSU-W1 T1 50 μm spinning disc) with a 20× air immersion objective. For instances where background RFP was consistently high, endogenous fluorescence was imaged without antibody amplification. For ovipositor images, flies were briefly anesthetized on CO₂ and the abdomen removed and embedded on slides with quick dry nail polish. Endogenous GFP was imaged with a 20× air immersion objective. All images were processed in ImageJ or Slidebook (3i software) and compiled in Adobe Illustrator. See the key resources table for more details.

Feeding assays Optogenetic PER

Flies were collected and placed on ATR or vehicle with normal food for two days. Flies were transferred to food-deprivation vials with 1% agar plus ATR or vehicle for one day prior to the assay as previously described. All vials were covered with foil to reduce light exposure and kept at 22°C. Flies were mounted for a labellar PER assay with mouth pipettes into 200 μ L pipette tips cut so only the heads were exposed. Flies were mounted in a dark room with minimal light under a dissection scope, allowed to recover in humidity chambers for \sim 1 h, and then water satiated. Water was presented as the first stimulus to ensure that flies did not PER to water, the second stimulus was a red LED powered by a 9V battery (emitting \sim 425 μ Watts) held directly over the labellum of the target fly. This stimulus was either given alone or in combination with 100 mM sucrose touched to the labellum. The final stimulus was 1 M sucrose as a positive control to ensure that the flies were still alive and able to respond. The water (always 0%) and 1 M sucrose (always 100%) were not included in the graphs.

Quantitative feeding assays

For optogenetic two-choice experiments, flies were exposed to ATR or vehicle as described above and kept at 25°C. Flies were mouth-pipetted directly into behavioral chambers that had two food options connected to capacitance sensors that quantified the number of interactions with each food source. One side triggered a red LED in individual chambers as the fly interacted with the corresponding food source. This was achieved by using either the opto-lid FlyPad system (STROBE)38,41 or the opto-lid FLIC system^{39,40} over 2 h. STROBE data were analyzed exactly as previously described.³⁸ The FLIC (Sable Systems) was used with the red opto-lid (signal threshold of 20 to active the LEDs, full code on GitHub) and data were analyzed similarly to previous publications to get the number of "interactions", "feeding events", and "feeding event duration". 39,40 For all FLIC two-choice assays, total interactions at the end of 2 h were computed and a preference index was calculated for each fly using ((interactions on side A - interactions on side B)/total interactions). One-choice optogenetic assays in the FLIC were performed as above with a green opto-lid programmed to be on continuously during the assay. FLIC assays without optogenetics were performed with standards lids (Sable Systems). For these experiments, flies were kept on regular food and flipped to 1% agar food-deprivation vials for one day before being loaded into the FLIC chambers. Each interaction on the food source was recorded for 3 h and the first 5 min were removed to exclude any artifacts that occurred while loading the flies. FLIC raw output was analyzed in custom R code based on that from the Pletcher Lab. Our feeding threshold signal was set to 20 and each 200 ms reading with this threshold counted as an interaction. For a feeding event, the signal must be present for at least 10 consecutive readings with gaps of inactivity less than or equal to 5 readings. Feeding durations for each event were quantified in seconds. In all experiments, flies of a particular genotype were varied by position in the Drosophila feeding monitor (DFM) boards and chambers each run. Any output that appeared to come from an error of the detection mechanism was removed, this included 0 signals or signals that were excessively high (>5000 interactions from raw data), and flies that failed to interact with a food source (<15 interactions), were removed. For FLIC data specifically, the background signal of a given chamber occasionally fluctuated, leading to a few flies with very high interactions (>3000) that may have been due to this artifact. We applied a ROUT outlier test to all FLIC data which identified and removed these significant outliers.

Dye-based assays

Groups of 10 flies were collected and kept on regular cornmeal food and flipped to 1% agar food-deprivation vials for one day prior to the two-choice assays. Binary choice assays were performed as previously described. ^{25,92} Briefly, vials contained six 10 μ L drops of alternating colors of dye mixed with indicated tastants in 1% agar with either blue (0.125 mg/mL Erioglaucine, FD and C Blue#1) or red (0.5 mg/mL Amaranth, FD and C Red#2) dye. Color was balanced so that half of the replicates had choice X in red, Y in blue, and half with Y in red, X in blue. Flies fed for 2 h at 29°C in the dark before freezing at -20°C. Abdomen color was scored under a dissection microscope as red, blue, purple, or no color. Preference index was calculated as ((# of flies labeled with X color)-(# of flies labeled with Y color))/(total # of flies with color). Any vials with <30% of flies feeding were excluded (very rare). The total number of flies eating either option was calculated as a percentage using ((# of flies labeled blue, red, or purple/total # flies in vial) *100).





Egg-laying assays

Groups of flies (12 females and 8 males) of indicated genotypes were collected and exposed to food and yeast paste for 48 h prior to the assay. Flies were transferred into empty bottles with a 35 mm Petri dish at the bottom containing indicated solutions in 1% agar, similar to previous protocols. ^{24,85} In one-choice assays, the same solution was distributed evenly across the plate, in two-choice assays, the agar solutions were cut in half and transferred carefully to a new dish. In experiments where male flies were removed, they were housed with the females for 48 h on food and yeast paste, and then all flies were briefly anesthetized to transfer only females into the egg-laying plates. CO₂ exposure was minimized to reduce its impact and genotype controls were also exposed. After 18 h in 25°C and 60% relative humidity, flies were anesthetized and counted. All embryos were manually counted under a dissection microscope. For two-choice assays, the preference index was calculated as ((# of eggs on capsaicin)-(# of eggs on vehicle))/(total # eggs).

Calcium imaging

In vivo imaging of GCaMP6f or GCaMP7f fluorescence of GRN terminals was performed as previously described (protocol document and video can be found in the Mendeley Data: http://www.doi.org/10.17632/d8bvxb3yfm.1). 25,30,92 Briefly, flies were lightly anesthetized on CO₂ and mounted in a custom chamber with the proboscis waxed in an extended position covering the maxillary palps. After 1 h of recovery in a humidity chamber, a small area of cuticle was removed, and a piece of the esophagus was cut to expose the SEZ. Adult hemolymph-like (AHL) solution (108 mM NaCl, 5 mM KCl, 4 mM NaHCO₃, 1 mM NaH₂PO₄, 5 mM HEPES, 15 mM ribose, 2 mM Ca²⁺, 8.2 mM Mg²⁺, pH 7.5) was continuously applied to the area and used for the immersion objective. A Leica SP5 II Confocal microscope was used to capture fluorescence with a 25× immersion objective, imaged at 4-6x zoom, 8000Hz line speed, line accumulation of 2, and a resolution of 512 x 512 pixels with the pinhole opened to 2.86 AU, as previously described. Tastants were delivered manually with a micromanipulator and a pulled capillary filed down to fit fully over the labellum. Each capture included 5 s of baseline, ~5 s of stimulus, and post-stimulus for a total of 15 s. The stimulator was washed in between different tastants, and a maximum of 5 tastants were given on any one fly with random order. For the screen of tastants (Figure 4A), data were collected on different sets of flies but combined in one graph for visualization purposes. In vivo imaging of GCaMP7f fluorescence in the axon terminals of the putative TPN in the SLP was performed as above with a few modifications. Two copies of UAS-iGCaMP7f were used to increase baseline fluorescence in these cells which required generating recombinant chromosomes to generate the following genotypes: UAS-jGCaMP7f/VT019729-AD; UAS-jGCaMP7f/VT008484-DBD, IR94e^{LexA} (LexA control), UAS-jGCaMP7f/ VT019729-AD; UAS-jGCaMP7f, LexAop-P2X2/VT008484-DBD (P2X2 control), UAS-jGCaMP7f/VT019729-AD; UAS-jGCaMP7f, LexAop-P2X2/VT008484-DBD, IR94e^{LexA} (experimental). Images were taken at 6x zoom, 8000Hz line speed, line accumulation of 4, pinhole opened to 209.95 μm, 10% laser power with 30% argon, and bidirectional acquisition. Each capture included 10 s of baseline, 5 s of stimulus, and post-stimulus for a total of 30 s. Due to the low baseline of GNG.SLP.T1 projections, a circular ROI with 30 µm diameter was consistently drawn 20 µm away from the nearby axon.

The baseline intensity for each video was calculated using 10 time points, and each time point was converted to the $\Delta F/F$ (%) using this baseline value. The maximum change in fluorescence (peak $\Delta F/F$) was calculated using the average of 3 time points during the stimulus period that showed peak intensity. ImageJ was used to quantify fluorescence changes and to create the heatmap using the 7df/f lookup table. As with our previous calcium imaging of IR94e neurons, occasionally we saw an unusually high-water response (>50%) in a small amount of flies (<15%), and those flies were removed from the analysis.

Connectomics analysis

IR94e neurons from both left and right hemisphere were identified on Codex (http://codex.flywire.ai, v630) based on morphology, predicted neurotransmitter expression, ⁴³ and public identification contributed by FlyWire community users. The morphological clustering was performed similarly to a previous report. ⁴⁸ IR94e neurons were compared with identified Gr64f neurons in the left hemisphere with the Navis 1.6.0 package in Python. NBLAST similarity scores were calculated and the NBLAST distance is 1 minus the similarity score. ⁴⁹ A dendrogram was generated for comparison. Ward's method was used for clustering and the dendrogram tree was cut at a distance of 1.0. OviDNs were identified based on morphology described in the original publication ⁵⁰ and the public identification contributed by FlyWire community users. The Connectivity pathways tool on Codex was used to identify the putative taste projection neurons and interneurons connecting IR94e neurons and OviDNs. Only connections with 3 or less hops were included in this analysis. The number of synapses between each set of neurons on the IR94e connectivity figure was also obtained from the pathway tool. The connectivity graph was plotted using Plotly graphing libraries in Python. The example pathway and projection neurons were visualized using 3D Render on Codex. Tables S1–S3 list the connectome neurons used in this study with the credits for individuals who contributed to the completion, identification, and more than 10% of proofreading edits for these cells. All lab heads associated with those credited were contacted about this manuscript more than one month before submission.

Fly Cell Atlas analysis

Using ASAP (https://flycellatlas.org),³¹ relevant tissue 10x stringent databases were cloned and filtered with pre-treatment cell filtering with the following QC parameters: More than 1000 UMI/reads, 1000 detected genes, and 80% protein coding genes and

Cell ReportsArticle



less than 20% mitochondrial genes and 40% ribosomal genes. Filtered cell sets were visualized via HVG_UMAP and individual positive cells were manually selected and expression values were recorded.

QUANTIFICATION AND STATISTICAL ANALYSIS

All statistical tests were performed in GraphPad Prism 10 software and included unpaired t-tests, one-way ANOVA with Dunnett's or Sidak's post tests, or two-way ANOVA with Dunnett's or Sidak's post tests. Specific tests for each experiment are stated in the figure legends along with sample sizes of biological replicates which were generally chosen based on variance and effect sizes seen in previous experiments using similar assays. Experimental or genotype controls were always run in parallel. Data are plotted as mean \pm SEM in all bar graphs and line graphs. As indicated in each figure legend, ns = p > .25, trending p values are indicated as there were some mild but consistent trends, and asterisks indicate p < 0.05, p < 0.01, p < 0.001, p < 0.0001.

Cell Reports, Volume 43

Supplemental information

Taste cells expressing *lonotropic Receptor 94e* reciprocally impact feeding and egg laying in *Drosophila*

Jacqueline Guillemin, Jinfang Li, Viktoriya Li, Sasha A.T. McDowell, Kayla Audette, Grace Davis, Meghan Jelen, Samy Slamani, Liam Kelliher, Michael D. Gordon, and Molly Stanley

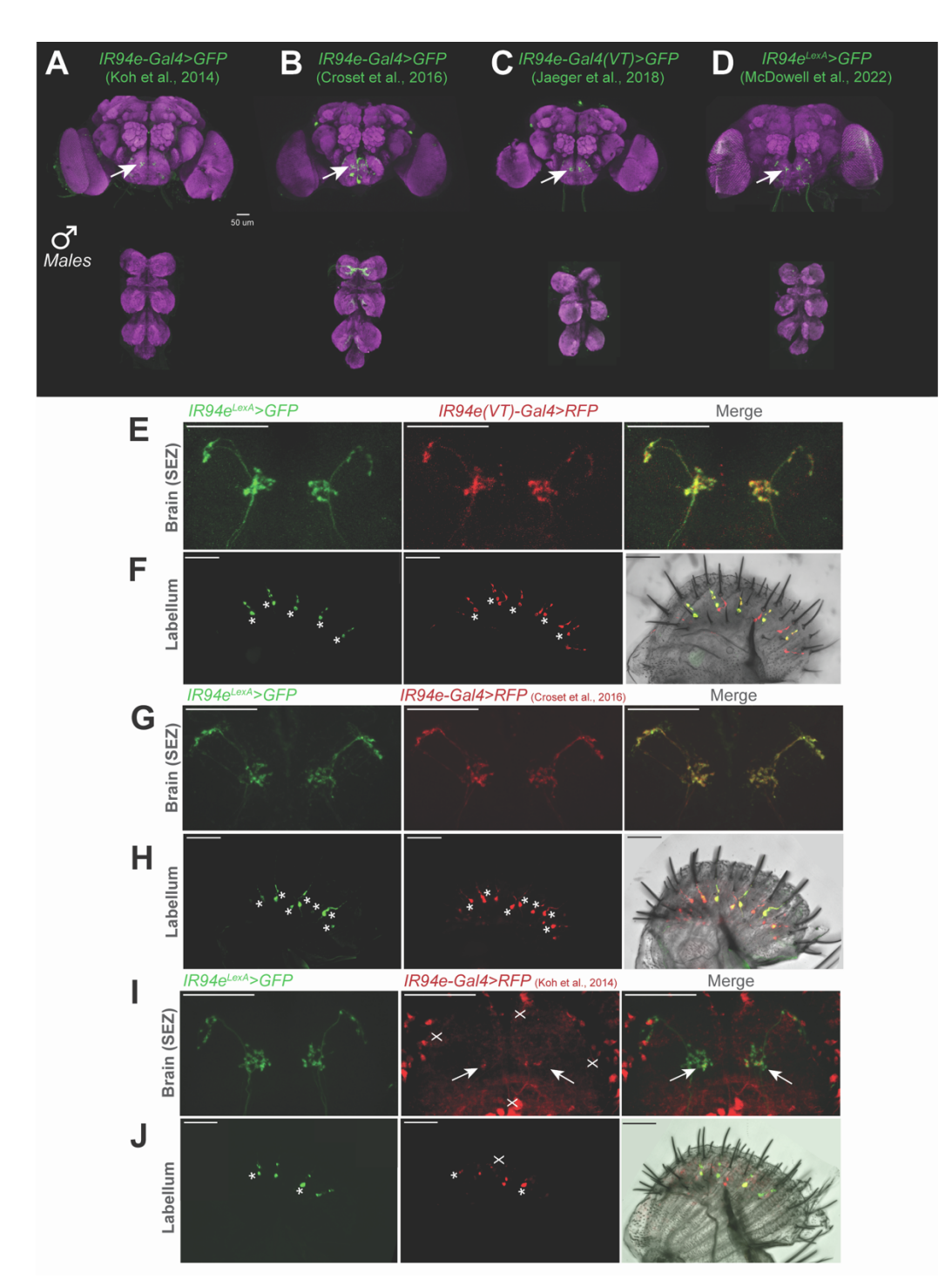


Figure S1. *IR94*e driver expression patterns are similar in males and label the same set of GRNs, Related to Figure 1

(**A-D**) Indicated driver lines expressing *UAS* or *LexAop mCD8::GFP*. Brain and VNC with neuropil and GFP staining in males, arrows indicate the specific pattern of axon terminals in the SEZ from labellar GRNs that is common across all lines. (**E-J**) $IR94e^{LEXA}$ driving GFP expression and indicated IR94e-Gal4 drivers expressing RFP in the brain SEZ (E, G, I) and labellum (F, H, J). White asterisks indicate neurons in L-type sensilla that overlap between both drivers. (**I,J**) The Koh et al., 2014 IR94e driver shows weak RFP with non-specific signal indicated by white "X" (compared to GFP expression in this line (S1A, 1A)), white arrows indicate specific RFP signal coming from the GRNs. All scale bars = 50 μ m.

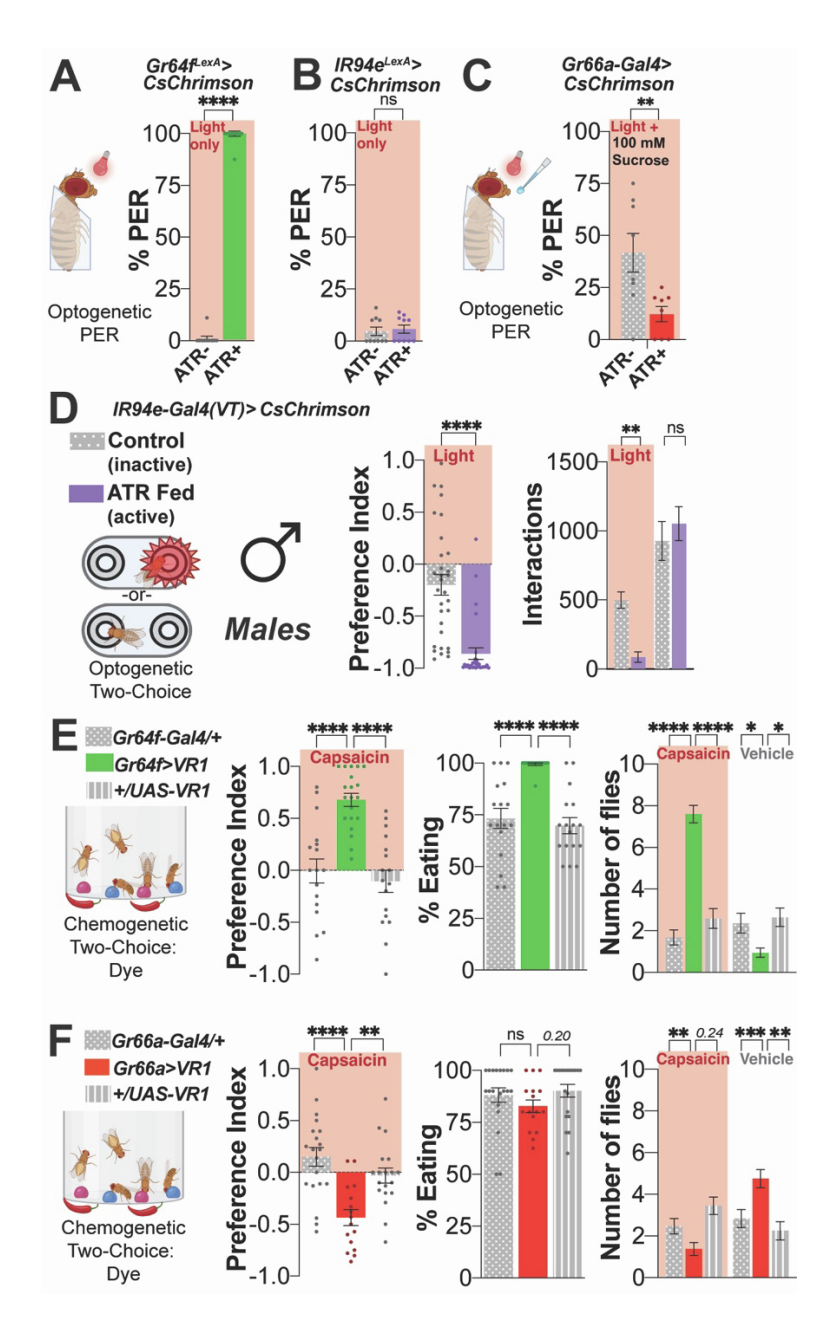


Figure S2. IR94e GRN activation produces feeding phenotypes that differ from canonical GRNs, Related to Figure 2

(**A-B**) Optogenetic activation of 'sweet' *Gr64f*+ GRNs (A) or IR94e GRNs (B) with light only, ATR (all-trans-retinal fed for active channels), n=10 groups of 6-10 flies per group. (**C**) Optogenetic activation of 'bitter' *Gr66a*+ GRNs with labellar sucrose stimulation to suppress PER, n=8 groups of 6-10 flies per group. (**D**) Optogenetic activation of IR94e GRNs in a two-choice chamber with 100 mM sucrose on both sides in male flies, n=29-31 flies per group. (**E-F**) Chemogenetic activation of 'sweet' *Gr64f*+ (E) or 'bitter' *Gr66a*+ (F) GRNs for comparison using VR1 and 100 μM capsaicin vs. vehicle (0.07% EtOH) in a dye-based, two-choice assay. Preference Index (left), total % of flies eating any option (middle), and number of flies consuming capsaicin vs. vehicle (right), n=16-20 groups of 10 flies. All mated females except D. All data plotted as mean +/- SEM. ns= p>.25, trending p values indicated, *p<.05, **p<.01, ***p<.001, *****p<.0001 by two-way ANOVA with Sidak's posttest (Number of flies and Interactions), one-way ANOVA with Dunnett's posttest (E, F Preference Index), or unpaired t-test (D Preference Index). Assay graphics created with Biorender.com

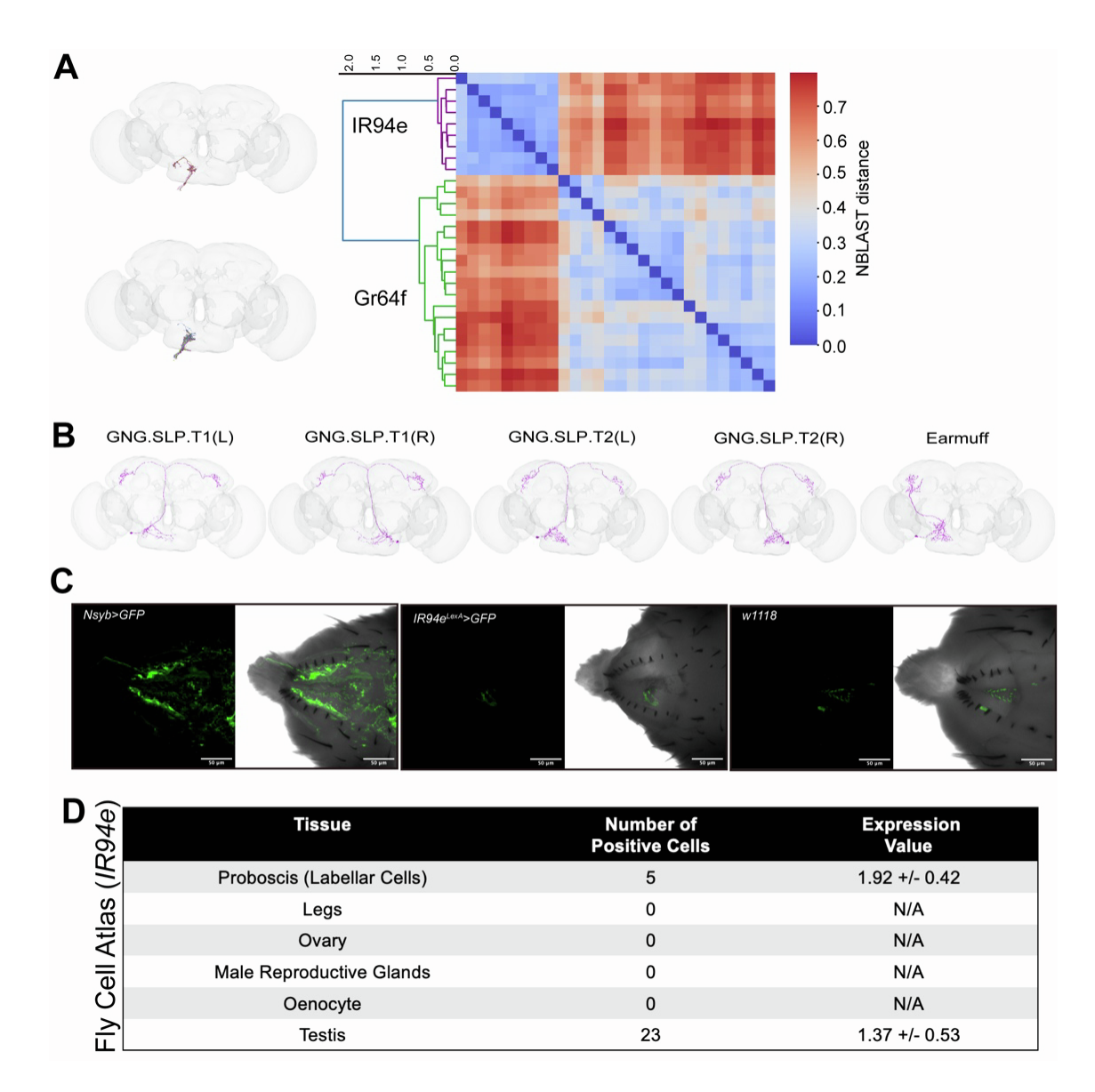


Figure S3: Labellar IR94e GRNs and putative TPNs identified in the connectome and IR94e expression in reproductive organs, Related to Figure 3

(A) IR94e and Gr64f GRNs identified in the left hemisphere in Codex (brains with identified neurons on the left) compared by morphological clustering to produce a dendrogram (scale on top left) along with an NBLAST distance matrix, plotted together for comparison. The Gr64f GRNs were identified based on the flywire community labels. Dendrogram tree was cut at the distance of 1.0. (B) Putative TPNs synapsing with IR94e GRNs as part of an oviposition circuit identified in FlyWire with their assigned names. (C) Ovipositor GFP alone and with brightfield, Nsyb-Gal4 is a positive control to label all neurons, w1118 is a negative control to account for autofluorescence. Scale bars = $50 \mu m$. (D) IR94e expression in taste and reproductive tissues from the Fly Cell Atlas database (https://flycellatlas.org), expression value listed as mean +/- SD.

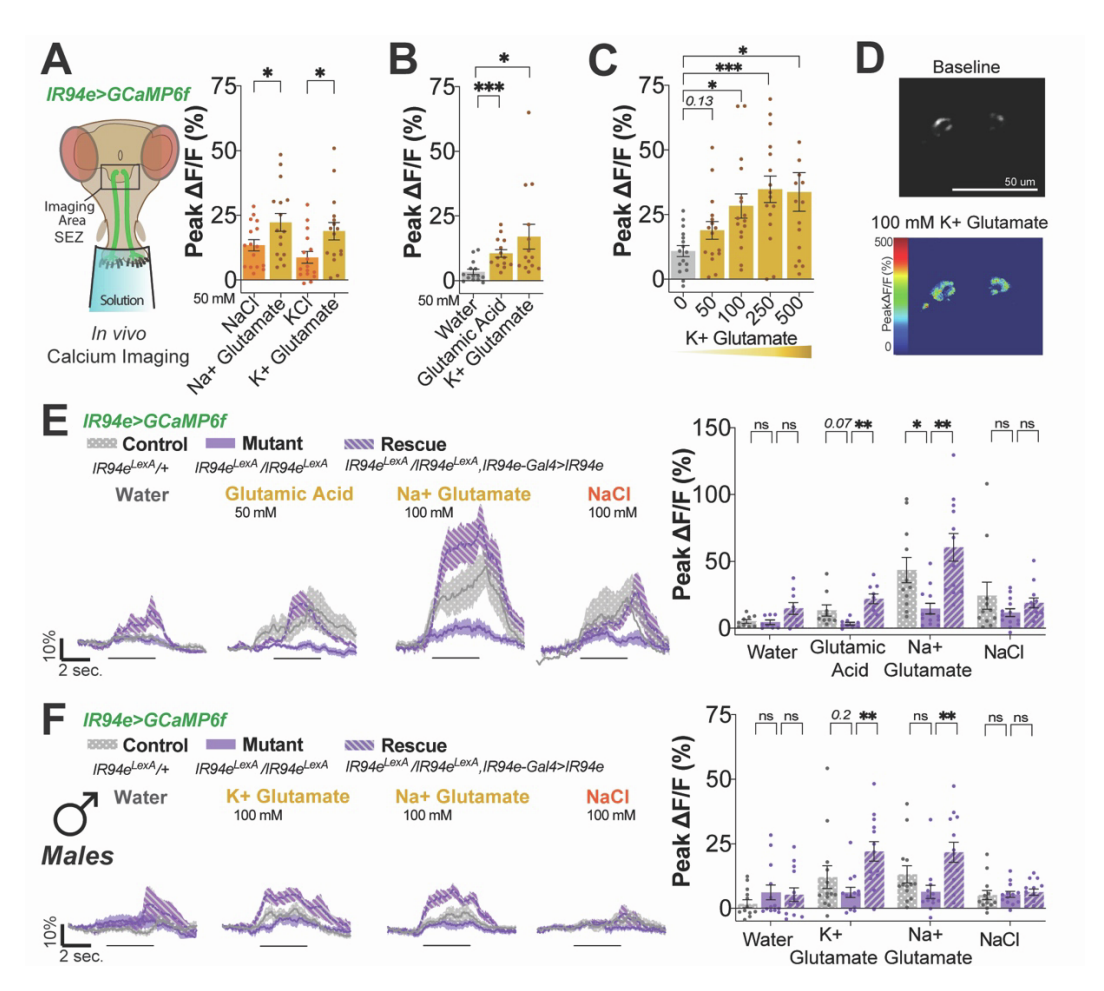


Figure S4. IR94e GRNs respond more strongly to glutamate than salt, Related to Figure 4 (A-C) *In vivo* calcium imaging peak fluorescent responses in IR94e GRNs with indicated solutions. (D) Heatmap showing GCaMP6f signal from IR94e projections in one representative fly at baseline and with glutamate stimulation, scale bars = $50 \mu m$ (E) Calcium imaging of IR94e GRNs in heterozygous controls, homozygous *IR94e* mutants, or *IR94e* mutants with *IR94e(VT)Gal4* driving *UAS-IR94e* (rescue). Fluorescent curves over time (left) and peak changes in fluorescence (right), n=8-13 flies per group. Black lines represent when the solution is over the labellum. (F) Same as (D) but in males. All data are plotted as mean +/- SEM. ns= p>.25, trending p values shown, *p<.05, **p<.01, ***p<.001, ****p<.0001 by oneway ANOVA with Sidak's (A) or Dunnett's (B) posttest, two-way ANOVA with Dunnett's posttest (D, E). All mated females except F.

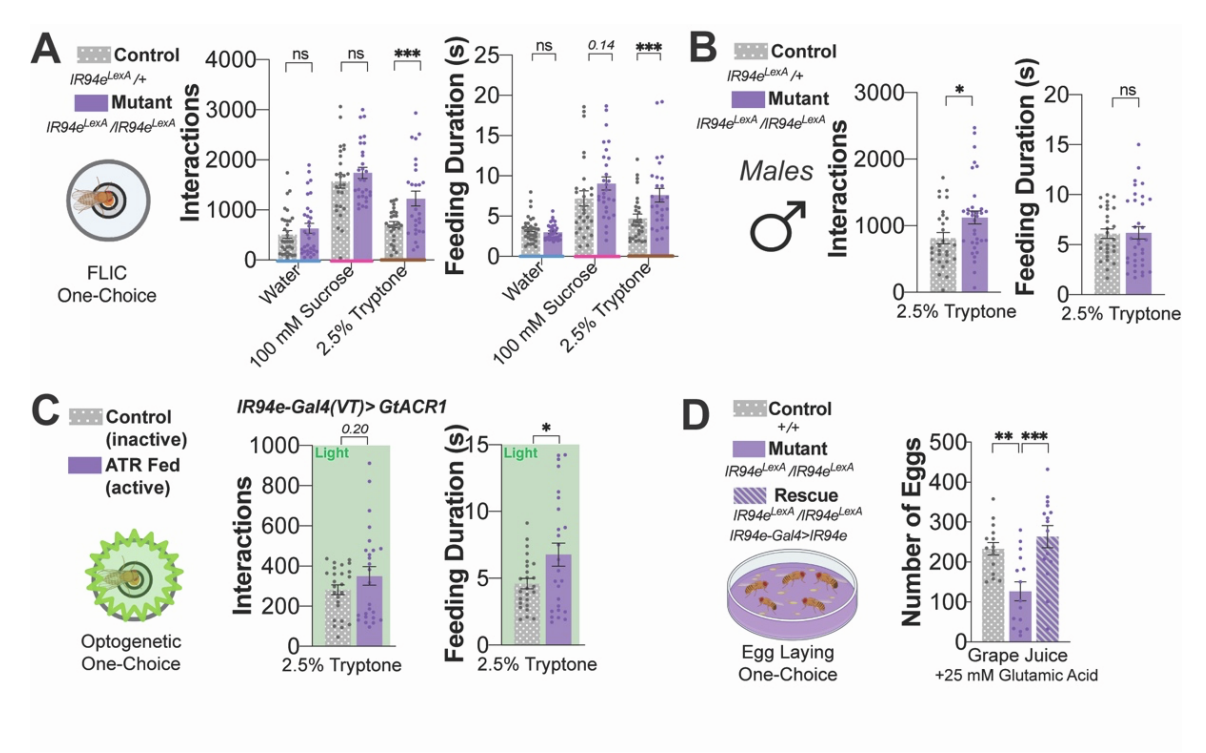


Figure S5. IR94e receptor and GRNs impact feeding and egg laying on amino acids, Related to Figure 5

(A) FLIC one-choice assay in mated females with indicated solutions in controls and *IR94e* mutants, n=26-33 flies per group. (B) FLIC one-choice assay in males with 2.5% tryptone in controls and *IR94e* mutants, n=24-28 flies. (C) Optogenetic silencing of IR94e GRNs in mated females, FLIC one-choice assay with 2.5% tryptone. Green opto-lids were on throughout the assay, ATR (all-*trans*-retinal fed for active channels), n=25-26 flies per group. (D) One-choice egg-laying assay on grape plates supplemented with glutamic acid in control, mutant, and rescue flies, n=13-15 groups of 12 females and 8 males. All data are plotted as mean +/- SEM. ns=not significant, *p<.05, **p<.01, ***p<.001 by unpaired t-test (B, C), one-way ANOVA with Dunnett's posttest (D), or two-way ANOVA with Sidak's posttest (A). Assay graphics created with Biorender.com.

Cell Name	Codex Link	ID	COMPLETION credits
IR94e	GNG.2013	720575940621375231	Ben Silverman
IR94e	GNG.2029	720575940638218173	Mendell Lopez
IR94e	GNG.2098	720575940626016017	Claire McKellar
IR94e	GNG.2040	720575940631082124	Christopher Dunne
IR94e	GNG.1981	720575940610683315	Claire McKellar
IR94e	GNG.2230	720575940612920386	J. Anthony Ocho
IR94e	GNG.2229	720575940614211295	Laia Serratosa
IR94e	<u>GNG.2153</u>	720575940624079544	Ben Silverman
IR94e	<u>GNG.2043</u>	720575940628198503	Christopher Dunne
IR94e	<u>GNG.2421</u>	720575940627438906	Christopher Dunne
IR94e	<u>GNG.2152</u>	720575940625450498	Christopher Dunne
IR94e	<u>GNG.2432</u>	720575940621898665	M Sorek
IR94e	<u>GNG.2315</u>	720575940627402568	Christopher Dunne
IR94e	<u>GNG.2586</u>	720575940643065032	Christopher Dunne
IR94e	<u>GNG.2340</u>	720575940611849178	Christopher Dunne
IR94e	<u>GNG.2726</u>	720575940637747519	Regine Salem
IR94e	GNG.2619	720575940625696601	Márcia Santos
IR94e	GNG.2292	720575940638813016	Christopher Dunne
GNG.SLP.T1 (L)	GNG.SLP.13	720575940624234254	Remer Tancontian, J. Anthony Ocho, Austin T Burke
GNG.SLP.T2 (L)	GNG.SLP.20	720575940619034782	Nash Hadjerol
GNG.SLP.T1 (R)	GNG.SLP.11	720575940616759014	Darrel Jay Akiatan, Irene Salgarella
GNG.SLP.T2 (R)	PRW.SLP.4	720575940623507273	Shirleyjoy Serona, Varun Sane, Rey Adrian Candilada
Earmuff	GNG.SLP.10	720575940631448874	Imaan Tamimi, Rey Adrian Candilada, Daril Bautista
Interneuron	SLP.SMP.32	720575940637878854	Zairene Lenizo
Interneuron	AVLP.SLP.36	720575940617406548	Kendrick Joules Vinson, Nash Hadjerol
Interneuron	AVLP.SLP.42	720575940628351217	Nash Hadjerol, Austin T Burke, Kendrick Joules Vinson
Interneuron	AVLP.SLP.9	720575940604516524	Nash Hadjerol, Darrel Jay Akiatan
Interneuron	SLP.SMP.67	720575940604395436	Rey Adrian Candilada, Jay Gager, Miguel Albero, Kendrick Joules Vinsont
Interneuron	<u>SLP.457</u>	720575940626446850	Austin T Burke, Imaan Tamimi, Remer Tancontian
Interneuron	SLP.52	720575940624247787	Varun Sane, Nash Hadjerol
Interneuron	SLP.378	720575940621569635	Zairene Lenizo
oviDN	SLP.FLA.8	720575940632512156	Katharina Eichler, Alexandre Javier
oviDN	SLP.FLA.3	720575940640872923	James Hebditch, Katharina Eichler, Alexandre Javier, Austin T Burke, Clyde
oviDN	SMP.FLA.45	720575940621257340	James Hebditch, Katharina Eichler, Alexandre Javier
oviDNa	SMP.FLA.13	720575940613316783	James Hebditch, Katharina Eichler, Alexandre Javier, Austin T Burke
oviDNa	SMP.VES.13	720575940642312136	Katharina Eichler, Alexandre Javier

Table S1. Completion credits for connectome neurons, Related to STAR Methods

Details of the connectome neurons used in this study and those credited with the completion of the reconstruction of these cells.

Cell Name	Codex Link	ID	IDENTIFICATION credits
IR94e	GNG.2013	720575940621375231	Greg Jefferis, Philip Shiu, Claire McKellar
IR94e	GNG.2029	720575940638218173	Philip Shiu
IR94e	GNG.2098	720575940626016017	Greg Jefferis, Philip Shiu, Claire McKellar
IR94e	GNG.2040	720575940631082124	Greg Jefferis, Philip Shiu, Claire McKellar, Christopher Dunne
IR94e	GNG.1981	720575940610683315	Philip Shiu
IR94e	GNG.2230	720575940612920386	Philip Shiu, Claire McKellar
IR94e	GNG.2229	720575940614211295	Greg Jefferis, Philip Shiu, Claire McKellar
IR94e	GNG.2153	720575940624079544	Greg Jefferis, Philip Shiu, Claire McKellar
IR94e	<u>GNG.2043</u>	720575940628198503	Greg Jefferis, Philip Shiu, Claire McKellar, Christopher Dunne
IR94e	GNG.2421	720575940627438906	Christopher Dunne
IR94e	GNG.2152	720575940625450498	Christopher Dunne
IR94e	GNG.2432	720575940621898665	
IR94e	GNG.2315	720575940627402568	Christopher Dunne
IR94e	GNG.2586	720575940643065032	Christopher Dunne
IR94e	GNG.2340	720575940611849178	Christopher Dunne, Claire McKellar
IR94e	GNG.2726	720575940637747519	Márcia Santos
IR94e	GNG.2619	720575940625696601	
IR94e	GNG.2292	720575940638813016	Christopher Dunne, Claire McKellar
GNG.SLP.T1 (L)	GNG.SLP.13	720575940624234254	
GNG.SLP.T2 (L)	GNG.SLP.20	720575940619034782	
GNG.SLP.T1 (R)	GNG.SLP.11	720575940616759014	Lab Members, Alexander Bates
GNG.SLP.T2 (R)	PRW.SLP.4	720575940623507273	Lab Members, Alexander Bates
Earmuff	GNG.SLP.10	720575940631448874	Lab Members, Alexander Bates, Philip Shiu
Interneuron	SLP.SMP.32	720575940637878854	
Interneuron	AVLP.SLP.36	720575940617406548	
Interneuron	AVLP.SLP.42	720575940628351217	
Interneuron	AVLP.SLP.9	720575940604516524	
Interneuron	SLP.SMP.67	720575940604395436	
Interneuron	<u>SLP.457</u>	720575940626446850	Lab Members, Alexander Bates, Kaiyu Wang, Dudi Deutsch
Interneuron	<u>SLP.52</u>	720575940624247787	Lab Members, Alexander Bates
Interneuron	<u>SLP.378</u>	720575940621569635	
oviDN	SLP.FLA.8	720575940632512156	Lab Members, Alexander Bates, Kaiyu Wang, Dudi Deutsch, Katharina Eichler
oviDN	SLP.FLA.3	720575940640872923	Lab Members, Alexander Bates, Kaiyu Wang, Dudi Deutsch, Katharina Eichler
oviDN	SMP.FLA.45	720575940621257340	Lab Members, Alexander Bates, Kaiyu Wang, Dudi Deutsch, Katharina Eichler
oviDNa	SMP.FLA.13	720575940613316783	Lab Members, Alexander Bates, Kaiyu Wang, Dudi Deutsch, Katharina Eichler
oviDNa	SMP.VES.13	720575940642312136	Lab Members, Alexander Bates, Kaiyu Wang, Dudi Deutsch, Katharina Eichler

Table S2. Identification credits for connectome neurons, Related to STAR Methods
Details of the connectome neurons used in this study and those credited with the identification of the reconstructed cells.

IR94e GNG.2029 720575940638218173 Mendell Lopez, Alexis E Santana Cruz IR94e GNG.2038 720575940626016017 Alexis E Santana Cruz, Claire McKellar IR94e GNG.2040 720575940631082124 Claire McKellar, Stefanie Hampel, Jinseor, Kim, Chan Hyuk Kang IR94e GNG.2030 720575940610683315 Claire McKellar, Chan Hyuk Kang, Alexis Galier McKellar, Chan Hyuk Kang, Cales Galier McKellar, Chan Hyu	Cell Name	Codex Link	ID	EDIT credits (>10% proofreading)
IR94e GNG.2098 720575940626016017 Alexis E Santana Cruz, Claire McKellar, IR94e GNG.2040 720575940631082124 Claire McKellar, Stefanie Hampel, Jinseor, Kim, Chan Hyuk Kang, IR94e GNG.1981 720575940610683315 Claire McKellar, Chan Hyuk Kang, Alexis Santana Cruz IR94e GNG.2229 720575940612920386 Jay Gager IR94e GNG.2229 720575940614211295 Claire McKellar, Chan Hyuk Kang, Alexis Santana Cruz, Laia Serratosa IR94e GNG.2153 720575940624079544 Claire McKellar, Chan Hyuk Kang, Alexis Santana Cruz, Laia Serratosa IR94e GNG.2043 720575940624079544 Claire McKellar, Chan Hyuk Kang, Alexis IR94e GNG.2043 720575940628198503 Alexis E Santana Cruz, Istvan Taisz, Jam Hebditch, Yijie Yin, Darrel Jay Akiatan IR94e GNG.2152 720575940627438906 Marcia Santos, Dhwani Patel, Chan Hyuk Kang IR94e GNG.2152 720575940627438906 Marcia Santos, Dhwani Patel, Chan Hyuk Kang IR94e GNG.2315 720575940627402568 Zhi Xi. Chan Hyuk Kang, hanetwo IR94e GNG.2315 720575940627402568 Zhi Xi. Chan Hyuk Kang, hanetwo IR94e GNG.2366 720575940637472519 Chan Hyuk Kang, Laire McKellar, Chan Hyuk Kang IR94e GNG.2361 72057594063747519 Chan Hyuk Kang, Zeba Vohra, Varun San IR94e GNG.2619 720575940625450601 Chira Nair, Marcia Santos IR94e GNG.2261 720575940625450601 Chira Nair, Marcia Santos IR94e GNG.2292 720575940638813016 Griffin Badalemente GNG.SLP.11 GNG.SLP.13 720575940631448874 Imaan Tamimi, Claire McKellar, Chan Hyuk Kang GNG.SLP.14 GNG.SLP.15 GNG.SLP.16 720575940631448874 Imaan Tamimi, Claire McKellar, Othira Nair, Marcia Santos IR94e GNG.2932 720575940631448874 Imaan Tamimi, Claire McKellar, Austin T Burke GNG.SLP.12 GNG.SLP.13 720575940631448874 Imaan Tamimi, Claire McKellar, Austin T Burke GNG.SLP.16 GNG.SLP.17 720575940631448874 Imaan Tamimi, Claire McKellar, Austin T Burke Interneuron AVLP.SLP.36 7205759406348351215 Austin T Burke Janua San, Janua San, Janua San, Janua San, Janu	IR94e	<u>GNG.2013</u>	720575940621375231	
IR94e GNG.2040 720575940631082124 Claire McKellar, Stefanie Hampel, Jinseor, Kin, Chan Hyuk Kang IR94e GNG.2230 720575940610683315 Claire McKellar, Chan Hyuk Kang, Alexis IR94e GNG.2229 720575940612920386 Jay Gager IR94e GNG.2229 720575940614211295 Claire McKellar, Chan Hyuk Kang, Alexis IR94e GNG.2153 720575940624079544 Claire McKellar, Chan Hyuk Kang, Alexis IR94e GNG.2043 720575940624079544 Claire McKellar, Chan Hyuk Kang, Alexis IR94e GNG.2043 720575940628198503 Alexis E Santana Cruz, Lala Serangel, Regine Sale IR94e GNG.2042 720575940628198503 Alexis E Santana Cruz, Lala Serangel, Regine Sale IR94e GNG.2042 720575940627438906 Alexis E Santana Cruz, Isvan Taisz, Jam Hebditch, Yije Yin, Darrel Jay Akiatan IR94e GNG.2152 720575940627438906 Márcia Santos, Dhwani Patel, Chan Hyuk Kang IR94e GNG.2152 720575940621898665 M Sorek, Chitra Nair, Chan Hyuk Kang IR94e GNG.2315 720575940621898665 M Sorek, Chitra Nair, Chan Hyuk Kang IR94e GNG.2364 720575940621898665 M Sorek, Chitra Nair, Chan Hyuk Kang IR94e GNG.2364 720575940630805032 Dharini Sapkal, Arti Yadav, Claire McKellar, IR94e GNG.2766 720575940637747519 Chan Hyuk Kang, Zeba Vohra, Varun San IR94e GNG.2766 720575940637747519 Chan Hyuk Kang, Zeba Vohra, Varun San IR94e GNG.2619 72057594063813016 Griffin Badalemente GNG.SLP.11 GNG.SLP.13 72057594063813016 Griffin Badalemente, Chitra Nair, Marcia Santos IR94e GNG.2619 7205759406394624234254 Griffin Badalemente, Chitra Nair GNG.SLP.11 720575940616759014 Irene Salgarella, Istvan Taisz, Mendell Logard Jay Akiatan GNG.SLP.12 720575940631448874 Irane Rajerol, Kendrick Joules Vinson Interneuron AVLP.SLP.94 720575940631448874 Irane Rajerol, Kendrick Joules Vinson Interneuron AVLP.SLP.94 720575940631448874 Irane Rajerol, Kendrick Joules Vinson Interneuron AVLP.SLP.94 720575940623507273 Griffin Badalemente, Varun Sane, Chitra Nair, Vijie Yi	IR94e	GNG.2029	720575940638218173	·
IR94e	IR94e	<u>GNG.2098</u>	720575940626016017	•
IR94e			720575940631082124	Kim, Chan Hyuk Kang
IR94e GNG.2229 720575940614211295 Claire McKellar, Chan Hyuk Kang, Alexis Santana Cruz, Laia Serratosa Cruz, Isvan Hyuk Kang, Alexis IR94e GNG.2043 720575940624079544 Claire McKellar, Chan Hyuk Kang, Alexis IR94e GNG.2043 720575940628198503 Alexis E Santana Cruz, Isvan Taisz, Jam Hebditch, Yijie Yin, Darrel Jay Akiatan IR94e GNG.2421 720575940627438906 Marcia Santos, Dhwani Patel, Chan Hyuk Kang IR94e GNG.2152 720575940625450498 Christopher Dunne IR94e GNG.2315 720575940627402568 ⊿lexis E Santana Cruz, Isvan Taisz, Jam Hebditch, Yijie Yin, Darrel Jay Akiatan IR94e GNG.2315 720575940627402568 ∆lexis E Santana Cruz, Isvan Patel, Chan Hyuk Kang IR94e GNG.2315 720575940627402568 ∆lexis Morek, Chitra Nair, Chan Hyuk Kang IR94e GNG.2315 720575940637402568 ∆lexis Morek, Chitra Nair, Chan Hyuk Kang IR94e GNG.2340 720575940634065032 Dharini Sapkal, Art Yadav, Claire McKellar IR94e GNG.2726 720575940637747519 Chan Hyuk Kang, Zeba Vohra, Varun San IR94e GNG.2726 720575940637747519 Chan Hyuk Kang, Zeba Vohra, Varun San IR94e GNG.292 720575940638813016 Chitra Nair, Márcia Santos GNG.292 720575940638813016 Chitra Nair, Márcia Santos GNG.SLP.11 GNG.SLP.13 720575940632434254 Remer Tancontian, Istvan Taisz, Philipp Schlegel, J. Anthony Ocho GNG.SLP.11 720575940616759014 Irene Salgarella, Istvan Taisz, Mendell Loj Darrel Jay Akiatan GNG.SLP.11 720575940633507273 Griffin Badalemente, Chitra Nair GNG.SLP.11 720575940631448874 Irene Salgarella, Istvan Taisz, Mendell Loj Darrel Jay Akiatan GNG.SLP.12 720575940631448874 Irene Salgarella, Istvan Taisz, Mendell Loj Darrel Jay Akiatan SLP.SMP.32 720575940631448874 Irene Salgarella, Istvan Taisz, Mendell Loj Darrel Jay Akiatan SLP.SMP.32 720575940631448874 Irene Salgarella, Istvan Taisz, Mendell Loj Darrel Jay Akiatan SLP.SMP.32 720575940631448874 Irene Salgarella, Istvan Taisz, Mendell Loj Darrel Jay Akiatan SLP.SMP.32 720575940634396346 Jay Gage				Santana Cruz
IR94e GNG.2153 720575940624079544 Silverman, Stefanie Hampel, Regine Sale IR94e GNG.2043 720575940628198503 Alexis E Santana Cruz, Istvan Taisz, Jama IR94e GNG.2421 720575940627438906 Márcia Santos, Dhwani Patel, Chan Hyuk Kang IR94e GNG.2421 720575940625450498 Christopher Dunne IR94e GNG.2432 720575940625450498 Christopher Dunne IR94e GNG.2315 720575940625450498 Christopher Dunne IR94e GNG.2315 720575940627402568 ½1 ½1 K, Chan Hyuk Kang IR94e GNG.2315 720575940627402568 ½1 ½1 K, Chan Hyuk Kang IR94e GNG.2340 720575940643065032 Dharini Sapkal, Arti Yadav, Claire McKellar (SNG.2586 720575940643065032 Dharini Sapkal, Arti Yadav, Claire McKellar (SNG.2566 720575940643065032 Dharini Sapkal, Arti Yadav, Claire McKellar (SNG.2566 720575940643065032 Dharini Sapkal, Arti Yadav, Claire McKellar (SNG.2566 720575940637747519 Chan Hyuk Kang, Zeba Vohra, Varun San IR94e GNG.2619 720575940637747519 Chan Hyuk Kang, Zeba Vohra, Varun San IR94e GNG.2292 720575940638813016 Griffin Badalemente GNG.SLP.11 GNG.SLP.13 720575940624234254 Remer Tancontian, Istvan Taisz, Philipp Schlegel, J. Anthony Ocho Darrel Jay Akidan GNG.SLP.11 720575940616759014 Irene Salgarella, Istvan Taisz, Mendell Lo Darrel Jay Akidan GNG.SLP.10 PRW.SLP.4 720575940633507273 Griffin Badalemente, Chitra Nair Interneuron SLP.SMP.32 720575940633813017 Salaelemente, Chitra Nair Interneuron AVLP.SLP.9 720575940633815217 Nash Hadjerol, Austin T Burke Interneuron AVLP.SLP.9 720575940633507273 Griffin Badalemente, Chitra Nair Interneuron AVLP.SLP.9 720575940633507273 Griffin Badalemente, Chitra Nair Interneuron SLP.SMP.67 720575940633512175 Nash Hadjerol, Austin T Burke Interneuron SLP.SLP.9 720575940633512175 Nash Hadjerol, Austin T Burke Interneuron SLP.SLP.9 72057594063495436 Jay Gager, Nash Hadjerol, Dahrain Sapka Interneuron SLP.547 72057594063495436 Jay Gager, Nash Hadjerol, Dahrain				
Silverman, Stefanie Hanpel, Regine Sale IR94e GNG.2043 720575940628198503 Alexis E Santana Cruzr, Istvan Taisz, Jam Hebditch, Yijie Yin, Darrel Jay Akiatan IR94e GNG.2421 720575940627438906 Márcia Santos, Dhwani Patel, Chan Hyuk Kang IR94e GNG.2152 720575940625450498 Christopher Dunne IR94e GNG.2432 720575940621898665 M Sorek, Chitra Nair, Chan Hyuk Kang IR94e GNG.2315 720575940627402568 Zhe, Chan Hyuk Kang, IR94e GNG.2586 72057594063032 Dharini Sapkal, Arti Yadav, Claire McKellar, Chan Hyuk Kang IR94e GNG.2340 720575940611849178 Claire McKellar, Chan Hyuk Kang IR94e GNG.2340 7205759406337747519 Chan Hyuk Kang, Zeba Vohra, Varun San IR94e GNG.2619 720575940625696601 Chitra Nair, Márcia Santos IR94e GNG.2619 720575940625696601 Chitra Nair, Márcia Santos IR94e GNG.2292 720575940624234254 Remer Tancontian, Istvan Taisz, Philipp GNG.SLP.71 (L) GNG.SLP.13 720575940619034782 Remer Tancontian, Istvan Taisz, Philipp GNG.SLP.72 (L) GNG.SLP.20 720575940619034782 Nash Hadjerol, Vijie Vin, James Hebditch, Griffin Badalemente, Chitra Nair GNG.SLP.72 (R) PRW.SLP.4 720575940638507273 Irene Salgarella, Istvan Taisz, Mendell Loj Darrel Jay Akiatan GNG.SLP.72 (R) PRW.SLP.4 720575940633507273 Irene Salgarella, Istvan Taisz, Mendell Loj Darrel Jay Akiatan Interneuron SLP.SMP.32 720575940637878854 Jay Gager, Nash Hadjerol, Norlain Salkan Interneuron SLP.SMP.32 7205759406395436 Jay Gager, Nash Hadjerol, Doharini Sapka Interneuron SLP.SMP.67 720575940624247787 Nash Hadjerol, Kendrick Joules Vinson Interneuron SLP.SMP.67 720575940624247787 Nash Hadjerol, Kendrick Joules Vinson Interneuron SLP.SMP.67 720575940624247787 Nash Hadjerol, Kendrick Joules Vinson Interneuron SLP.SMP.67 720575940624247787 Varun Sane, Chitra Nair, Yijie Yin, Yashvi Interneuron SLP.SA2 720575940624247787 Varun Sane, Chitra Nair, Yijie Yin, Yashvi Interneuron SLP.SA37 7205759406242477				Santana Cruz, Laia Serratosa
Hebditch, Yijie Yin, Darrel Jay Akiatan IR94e GNG_2421 720575940627438906 Márica Santos, Dhwani Patel, Chan Hyuk Kang IR94e GNG_2432 720575940625450498 Christopher Dunne IR94e GNG_2432 720575940621898665 M Sorek, Chitra Nair, Chan Hyuk Kang IR94e GNG_2315 720575940627402568 건전				Silverman, Stefanie Hampel, Regine Salem
R94e GNG.2152 720575940625450498 Christopher Dunne IR94e GNG.2432 720575940621898665 M Sorek, Chitra Nair, Chan Hyuk Kang IR94e GNG.2315 720575940627402568 길진성, Chan Hyuk Kang, hanetwo IR94e GNG.2586 720575940643065032 Dharini Sapkal, Arti Yadav, Claire McKellar IR94e GNG.2340 720575940611849178 Claire McKellar, Chan Hyuk Kang IR94e GNG.2340 720575940611849178 Claire McKellar, Chan Hyuk Kang IR94e GNG.2340 720575940637747519 Chan Hyuk Kang, Zeba Vohra, Varun San IR94e GNG.2619 720575940625696601 Chitra Nair, Márcia Santos IR94e GNG.2292 720575940638813016 Griffin Badalemente GNG.SLP.T1 (L) GNG.SLP.13 720575940624234254 Remer Tancontian, Istvan Taisz, Philipp GNG.SLP.T2 (L) GNG.SLP.20 720575940619034782 Nash Hadjerol, Yijie Yin, James Hebditch, Griffin Badalemente, Chitra Nair GNG.SLP.T2 (R) PRW.SLP.4 720575940616759014 Irene Salgarla, Istvan Taisz, Mendell Lol Darrel Jay Akiatan GNG.SLP.T2 (R) PRW.SLP.4 720575940633507273 Griffin Badalemente, Varun Sane, Chitra Nair GNG.SLP.T1 720575940633507273 Griffin Badalemente, Varun Sane, Chitra Nair Interneuron SLP.SMP.32 720575940631448874 Imaan Tamimi, Claire McKellar, Dharini Surka Interneuron AVLP.SLP.36 720575940633507273 Zairene Lenizo, Claire McKellar, Austin T Burke Interneuron AVLP.SLP.94 72057594063351217 Nash Hadjerol, Kendrick Joules Vinson Interneuron SLP.SMP.67 720575940623507273 Jay Gager, Nash Hadjerol, Dharini Sapka Interneuron SLP.SMP.67 720575940624247787 Varun Sane, Chitra Nair, Yijie Yin, Yashvi Interneuron SLP.378 720575940624247787 Varun Sane, Chitra Nair, Yijie Yin, Yashvi Interneuron SLP.378 720575940624247787 Varun Sane, Chitra Nair, Yijie Yin, Yashvi Interneuron SLP.378 720575940624247787 Varun Sane, Chitra Nair, Yijie Yin, Yashvi Interneuron SLP.378 7205759406212569635 Austin T Burke, Joshua SMP.FLA.45 720575940621257340 Varun Sane, A. Javier OviDN SMP.F				Hebditch, Yijie Yin, Darrel Jay Akiatan
IR94e GNG.2432 720575940621898665 M Sorek, Chitra Nair, Chan Hyuk Kang IR94e GNG.2315 720575940627402568 21 전 Chan Hyuk Kang, hanetwo IR94e GNG.2586 720575940643065032 Dharini Sapkal, Arti Yadav, Claire McKellar IR94e GNG.2340 720575940611849178 Claire McKellar, Chan Hyuk Kang IR94e GNG.2726 720575940637747519 Chan Hyuk Kang, Zeba Vohra, Varun San IR94e GNG.2619 720575940625696601 Chitra Nair, Maricai Santos IR94e GNG.2619 720575940625696601 Chitra Nair, Maricai Santos IR94e GNG.2292 720575940638813016 Griffin Badalemente GNG.SLP.T1 (L) GNG.SLP.13 720575940624234254 Remer Tancontian, Istvan Taisz, Philipp Schlegel, J. Anthony Ocho GNG.SLP.T2 (L) GNG.SLP.20 720575940619034782 Nash Hadjerol, Yije Yin, James Hebditch, Griffin Badalemente, Chitra Nair Griffin Badalemente, Varun Sane, Chitra I Dhwani Patel Earmuff GNG.SLP.11 720575940623507273 Griffin Badalemente, Varun Sane, Chitra I Dhwani Patel Earmuff GNG.SLP.10 720575940631448874 Imaan Tamimi, Claire McKellar, Dharini St Interneuron SLP.SMP.32 720575940623507273 Sairene Lenizo, Claire McKellar, Dharini St Interneuron AVLP.SLP.36 720575940637878854 Zairene Lenizo, Claire McKellar, Dharini St Interneuron AVLP.SLP.36 720575940628351217 Nash Hadjerol, Kendrick Joules Vinson Interneuron AVLP.SLP.9 720575940628351217 Nash Hadjerol, Austin T Burke, Joshua Ba Interneuron SLP.SMP.67 720575940624247787 Varun Sane, Chitra Nair, Yijie Yin, Yashvi Interneuron SLP.378 720575940624247787 Varun Sane, Chitra Nair, Yijie Yin, Yashvi Interneuron SLP.378 720575940624247787 Varun Sane, Chitra Nair, Yijie Yin, Yashvi Interneuron SLP.378 720575940621559635 Austin T Burke, Varun Sane, Katharina Ei OviDN SLP.FLA.8 720575940621557340 Varun Sane, A. Javier OviDN SMP.FLA.45 720575940631316783 Vijie Yin, Arti Yadav, Márcia Santos, Zhiha oviDNa SMP.FLA.413 720575940631316783 Vijie Yin, Arti Yadav, Márcia Santos, Zhiha oviDNa SMP.FLA.4	IR94e	GNG.2421	720575940627438906	Kang
IR94e GNG.2315 720575940627402568 권선, Chan Hyuk Kang, hanetwo IR94e GNG.2586 720575940643065032 Dharini Sapkal, Arti Yadav, Claire McKellar IR94e GNG.2340 720575940611849178 Claire McKellar, Chan Hyuk Kang IR94e GNG.2726 720575940637747519 Chan Hyuk Kang, Zeba Vohra, Varun San IR94e GNG.2619 720575940625696601 Chitra Nair, Márcia Santos IR94e GNG.2292 720575940625696601 Chitra Nair, Márcia Santos IR94e GNG.2292 720575940624234254 Remer Tancontian, Istvan Taisz, Philipp Schlegel, J. Anthony Ocho GNG.SLP.T1 (L) GNG.SLP.13 720575940619034782 Remer Tancontian, Istvan Taisz, Philipp Schlegel, J. Anthony Ocho GNG.SLP.T2 (L) GNG.SLP.20 720575940619034782 Remer Tancontian, Istvan Taisz, Mendell Loj GNG.SLP.T1 Royal Royal Royal Remer Tancontian, Istvan Taisz, Mendell Loj Darrel Jay Akiatan GNG.SLP.11 720575940616759014 Irene Salgarella, Istvan Taisz, Mendell Loj Darrel Jay Akiatan GNG.SLP.11 720575940623507273 Griffin Badalemente, Varun Sane, Chitra Nair Ireneuron SLP.SMP.32 720575940631448874 Irena Tamimi, Claire McKellar, Austin T Burke Interneuron AVLP.SLP.36 720575940637878854 Zairene Lenizo, Claire McKellar, Austin T Burke Interneuron AVLP.SLP.36 720575940628351217 Nash Hadjerol, Austin T Burke, Joshua Balanterneuron AVLP.SLP.9 720575940624516524 Jay Gager, Nash Hadjerol, Dharini Sapka Interneuron SLP.37 720575940624247787 Varun Sane, Chitra Nair, Yijie Yin, Yashvi Interneuron SLP.37 720575940624247787 Varun Sane, Chitra Nair, Yijie Yin, Yashvi Interneuron SLP.37 720575940621569635 Austin T Burke OviDN SLP.FLA.8 720575940621569635 Austin T Burke, Varun Sane, Katharina Ei OviDN SLP.FLA.3 720575940621257340 Varun Sane, A. Javier OviDN SMP.FLA.45 72057594062136783 Vijie Yin, Arti Yadav, Márcia Santos, Zhiha OviDNa SMP.FLA.43 720575940613316783 Vijie Yin, Arti Yadav, Márcia Santos, Zhiha OviDNa SMP.FLA.43 720575940613316783 Vijie Yi				<u> </u>
IR94e GNG.2586 720575940643065032 Dharini Sapkal, Arti Yadav, Claire McKellar IR94e GNG.2340 720575940611849178 Claire McKellar, Chan Hyuk Kang IR94e GNG.2726 720575940637747519 Chan Hyuk Kang, Zeba Vohra, Varun San IR94e GNG.2619 720575940625696601 Chitra Nair, Márcia Santos IR94e GNG.2292 720575940625696601 Chitra Nair, Márcia Santos IR94e GNG.2292 720575940638813016 Griffin Badalemente GNG.SLP.T1 (L) GNG.SLP.13 720575940624234254 Remer Tancontian, Istvan Taisz, Philipp Schlegel, J. Anthony Ocho SNG.SLP.T2 (L) GNG.SLP.20 720575940619034782 Nash Hadjerol, Yijie Yin, James Hebditch, Griffin Badalemente, Chitra Nair Irene Salgarella, Istvan Taisz, Mendell Loj Darrel Jay Akiatan GNG.SLP.T1 (R) GNG.SLP.11 720575940616759014 Irene Salgarella, Istvan Taisz, Mendell Loj Darrel Jay Akiatan GNG.SLP.T2 (R) PRW.SLP.4 720575940623507273 Griffin Badalemente, Varun Sane, Chitra Nair Interneuron SLP.SMP.32 720575940631448874 Imaan Tamimi, Claire McKellar, Austin T Burke Interneuron AVLP.SLP.36 720575940617406548 Nash Hadjerol, Kendrick Joules Vinson Interneuron AVLP.SLP.36 720575940628351217 Nash Hadjerol, Austin T Burke Interneuron SLP.SMP.67 720575940628351217 Nash Hadjerol, Austin T Burke Interneuron SLP.SMP.67 72057594062446850 Austin T Burke Jay Gager, Nash Hadjerol, Dharini Sapka Interneuron SLP.SMP.67 72057594062446850 Austin T Burke Jay Gager, Austin T Burke Interneuron SLP.378 72057594062447787 Varun Sane, Chitra Nair, Yijie Yin, Yashvi Interneuron SLP.378 720575940621569635 Austin T Burke OviDN SLP.FLA.8 720575940621567340 Jay Gager, Austin T Burke OviDN SMP.FLA.45 720575940613316783 Varun Sane, A. Javier OviDN SMP.FLA.41 720575940613316783		<u>GNG.2432</u>	720575940621898665	M Sorek, Chitra Nair, Chan Hyuk Kang
IR94e GNG.2340 720575940611849178 Claire McKellar, Chan Hyuk Kang IR94e GNG.2726 720575940637747519 Chan Hyuk Kang, Zeba Vohra, Varun San IR94e GNG.2619 720575940625696601 Chitra Nair, Márcia Santos IR94e GNG.2292 720575940628813016 Griffin Badalemente GNG.SLP.T1 (L) GNG.SLP.13 720575940624234254 Remer Tancontian, Istvan Taisz, Philipp Schlegel, J. Anthony Ocho SLP.SLP.20 720575940619034782 Remer Tancontian, Istvan Taisz, Philipp Schlegel, J. Anthony Ocho SLP.SLP.21 720575940619034782 Remer Tancontian, Istvan Taisz, Philipp Schlegel, J. Anthony Ocho SLP.SLP.21 720575940619034782 Remer Tancontian, Istvan Taisz, Philipp Schlegel, J. Anthony Ocho SLP.SLP.20 720575940619034782 Remer Tancontian, Istvan Taisz, Philipp Schlegel, J. Anthony Ocho SLP.SLP.20 720575940624234254 Remer Tancontian, Istvan Taisz, Philipp Schlegel, J. Anthony Ocho SLP.SLP.20 720575940619034782 Remer Tancontian, Istvan Taisz, Philipp Schlegel, J. Anthony Ocho SLP.SLP.20 720575940619034782 Irene Salgarella, Istvan Taisz, Mendell Lop Darrel Jay Akiatan Irene Salgarella, Istvan Taisz, Mendell Lop Darrel Jay Akiatan Irene Salgarella, Istvan Taisz, Mendell Lop Darrel Jay Akiatan Irene Lenizo, Claire McKellar, Dharini Stair Interneuron SLP.SMP.32 720575940631448874 Imaan Tamimi, Claire McKellar, Dharini Staire Lenizo, Claire McKellar, Austin T Burke Interneuron AVLP.SLP.36 720575940628351217 Nash Hadjerol, Kendrick Joules Vinson Interneuron AVLP.SLP.36 720575940624351217 Nash Hadjerol, Austin T Burke Interneuron SLP.SMP.67 720575940626446850 Jay Gager, Austin T Burke Interneuron SLP.378 72057594062424247787 Varun Sane, Chitra Nair, Yijie Yin, Yashvi Interneuron SLP.378 720575940632512156 Austin T Burke, Varun Sane, Katharina Ei OviDN SLP.FLA.3 720575940640872923 Joseph Hsu, Greg Jefferis OviDN SMP.FLA.45 720575940613316783 Yijie Yin, Arti Yadav, Márcia Santos, Zhiha OviDNa SM	IR94e	<u>GNG.2315</u>	720575940627402568	김진성, Chan Hyuk Kang, hanetwo
IR94e GNG.2726 720575940637747519 Chan Hyuk Kang, Zeba Vohra, Varun San IR94e GNG.2619 720575940625696601 Chitra Nair, Márcia Santos IR94e GNG.2292 720575940638813016 Griffin Badalemente GNG.SLP.T1 (L) GNG.SLP.13 720575940624234254 Remer Tancontian, Istvan Taisz, Philipp Schlegel, J. Anthony Ocho GNG.SLP.T2 (L) GNG.SLP.20 720575940619034782 Remer Tancontian, Istvan Taisz, Philipp Schlegel, J. Anthony Ocho SLP.SLP.11 720575940619034782 Nash Hadjerol, Yijie Yin, James Hebditch, Griffin Badalemente, Chitra Nair GNG.SLP.T1 (R) GNG.SLP.11 720575940616759014 Irene Salgarella, Istvan Taisz, Mendell Loj Darrel Jay Akiatan GNG.SLP.T2 (R) PRW.SLP.4 720575940623507273 Griffin Badalemente, Varun Sane, Chitra Nair Dhwani Patel Earmuff GNG.SLP.10 7205759406314448874 Imaan Tamimi, Claire McKellar, Dharini Sale Interneuron SLP.SMP.32 720575940637878854 Zairene Lenizo, Claire McKellar, Dharini Sale Interneuron AVLP.SLP.36 720575940617406548 Nash Hadjerol, Kendrick Joules Vinson Interneuron AVLP.SLP.9 720575940628351217 Nash Hadjerol, Austin T Burke, Joshua Balanterneuron SLP.SMP.67 720575940604516524 Jay Gager, Nash Hadjerol, Dharini Sapka Interneuron SLP.SMP.67 72057594062446850 Jay Gager, Austin T Burke Interneuron SLP.378 720575940624447787 Varun Sane, Chitra Nair, Yijie Yin, Yashvi Interneuron SLP.378 720575940632512156 Austin T Burke Varun Sane, Katharina Ei oviDN SLP.FLA.8 720575940640872923 Joseph Hsu, Greg Jefferis OviDN SLP.FLA.45 720575940613316783 Yijie Yin, Arti Yadav, Márcia Santos, Zhiha OviDNa SMP.FLA.13 720575940613316783 Yijie Yin, Arti Yadav, Márcia Santos, Zhiha OviDNa SMP.FLA.13 720575940613316783 Yijie Yin, Arti Yadav, Márcia Santos, Zhiha OviDNa SMP.FLA.13 720575940613316783 Yijie Yin, Arti Yadav, Márcia Santos, Zhiha OviDNa SMP.FLA.13 720575940613316783 Yijie Yin, Arti Yadav, Márcia Santos, Zhiha OviDNa SMP.FLA.13 7205759406133167	IR94e	GNG.2586	720575940643065032	Dharini Sapkal, Arti Yadav, Claire McKellar
IR94e GNG.2619 720575940625696601 Chitra Nair, Márcia Santos IR94e GNG.2292 720575940638813016 Griffin Badalemente GNG.SLP.T1 (L) GNG.SLP.13 720575940624234254 Remer Tancontian, Istvan Taisz, Philipp Schlegel, J. Anthony Ocho GNG.SLP.T2 (L) GNG.SLP.20 720575940619034782 Nash Hadjerol, Yijie Yin, James Hebditch, Griffin Badalemente, Chitra Nair GNG.SLP.T1 (R) GNG.SLP.11 720575940616759014 Irene Salgarella, Istvan Taisz, Mendell Loparrel Jay Akiatan GNG.SLP.T2 (R) PRW.SLP.4 720575940623507273 Griffin Badalemente, Varun Sane, Chitra Nair Earmuff GNG.SLP.10 720575940631448874 Imaan Tamimi, Claire McKellar, Dharini Starke Interneuron SLP.SMP.32 720575940637878854 Zairene Lenizo, Claire McKellar, Austin Taurke Interneuron AVLP.SLP.36 720575940617406548 Nash Hadjerol, Kendrick Joules Vinson Interneuron AVLP.SLP.42 720575940628351217 Nash Hadjerol, Austin Taurke Interneuron SLP.SMP.67 720575940604516524 Jay Gager, Nash Hadjerol, Dharini Sapka Interneuron SLP.SMP.67 72057594062495436 Jay Gager, Austin Taurke Interneuron SLP.457 720575940624247787 Varun Sane, Chitra Nair, Yijie Yin, Yashvi Interneuron SLP.378 720575940624247787 Varun Sane, Chitra Nair, Yijie Yin, Yashvi Interneuron SLP.52 720575940624247787 Varun Sane, Chitra Nair, Yijie Yin, Yashvi Interneuron SLP.58 720575940624247787 Varun Sane, Chitra Nair, Yijie Yin, Yashvi Interneuron SLP.58 720575940624247787 Varun Sane, Chitra Nair, Yijie Yin, Yashvi Interneuron SLP.54 720575940624257340 Varun Sane, Chitra Nair, Yijie Yin, Yashvi OviDN SLP.FLA.3 720575940621257340 Varun Sane, A. Javier OviDN SMP.FLA.45 720575940613316783 Yijie Yin, Arti Yadav, Márcia Santos, Zhiha	IR94e	GNG.2340	720575940611849178	
IR94e GNG.2292 720575940638813016 Griffin Badalemente	IR94e	GNG.2726	720575940637747519	Chan Hyuk Kang, Zeba Vohra, Varun Sane
GNG.SLP.T1 (L) GNG.SLP.13 T20575940624234254 Remer Tancontian, Istvan Taisz, Philipp Schlegel, J. Anthony Ocho GNG.SLP.T2 (L) GNG.SLP.20 T20575940619034782 Nash Hadjerol, Yijie Yin, James Hebditch, Griffin Badalemente, Chitra Nair GNG.SLP.T1 (R) GNG.SLP.11 T20575940616759014 Irene Salgarella, Istvan Taisz, Mendell Lop Darrel Jay Akiatan GNG.SLP.T2 (R) PRW.SLP.4 T20575940623507273 Griffin Badalemente, Varun Sane, Chitra Nair Earmuff GNG.SLP.10 T20575940631448874 Imaan Tamimi, Claire McKellar, Dharini Saler Interneuron SLP.SMP.32 SLP.SMP.32 T20575940637878854 Interneuron AVLP.SLP.36 Interneuron AVLP.SLP.36 AVLP.SLP.36 AVLP.SLP.37 AVLP.SLP.39 Interneuron SLP.SMP.67 T20575940626451524 Jay Gager, Nash Hadjerol, Dharini Sapka Interneuron SLP.SMP.67 T20575940626446850 Interneuron SLP.457 T20575940626446850 Austin T Burke, Varun Sane, J. Anthony Cohara Kakadiya Interneuron SLP.378 T20575940624247787 Varun Sane, Chitra Nair, Yijie Yin, Yashvi Interneuron SLP.378 T20575940640872923 Joseph Hsu, Greg Jefferis oviDN SLP.FLA.3 T2057594061257340 Varun Sane, A. Javier oviDNa SMP.FLA.45 T20575940613316783 Yijie Yin, Arti Yadav, Márcia Santos, Zhiha	IR94e	<u>GNG.2619</u>	720575940625696601	Chitra Nair, Márcia Santos
Schlegel, J. Anthony Ocho	IR94e	GNG.2292	720575940638813016	Griffin Badalemente
Griffin Badalemente, Chitra Nair	GNG.SLP.T1 (L)	GNG.SLP.13	720575940624234254	
Darrel Jay Akiatan	, ,	GNG.SLP.20	720575940619034782	
Dhwani Patel	` ′	GNG.SLP.11	720575940616759014	
Interneuron SLP.SMP.32 720575940637878854 Zairene Lenizo, Claire McKellar, Austin T Burke Interneuron AVLP.SLP.36 720575940617406548 Nash Hadjerol, Kendrick Joules Vinson Interneuron AVLP.SLP.42 720575940628351217 Nash Hadjerol, Austin T Burke, Joshua Ba Interneuron AVLP.SLP.9 720575940604516524 Jay Gager, Nash Hadjerol, Dharini Sapka Interneuron SLP.SMP.67 720575940604395436 Jay Gager, Austin T Burke Interneuron SLP.457 720575940626446850 Austin T Burke, Varun Sane, J. Anthony On Dhara Kakadiya Interneuron SLP.52 720575940624247787 Varun Sane, Chitra Nair, Yijie Yin, Yashvi Interneuron SLP.378 720575940621569635 Austin T Burke oviDN SLP.FLA.8 720575940632512156 Austin T Burke, Varun Sane, Katharina Einer oviDN SLP.FLA.3 720575940640872923 Joseph Hsu, Greg Jefferis oviDN SMP.FLA.45 720575940621257340 Varun Sane, A. Javier oviDNa SMP.FLA.13 720575940613316783 Yijie Yin, Arti Yadav, Márcia Santos, Zhiha	GNG.SLP.T2 (R)	PRW.SLP.4	720575940623507273	
Interneuron	Earmuff	GNG.SLP.10	720575940631448874	Imaan Tamimi, Claire McKellar, Dharini Sapkal
Interneuron AVLP.SLP.42 720575940628351217 Nash Hadjerol, Austin T Burke, Joshua Ballaterneuron Interneuron AVLP.SLP.9 720575940604516524 Jay Gager, Nash Hadjerol, Dharini Sapka Interneuron SLP.SMP.67 720575940604395436 Jay Gager, Austin T Burke Interneuron SLP.457 720575940626446850 Austin T Burke, Varun Sane, J. Anthony Control Dhara Kakadiya Interneuron SLP.52 720575940624247787 Varun Sane, Chitra Nair, Yijie Yin, Yashvi Interneuron SLP.378 720575940621569635 Austin T Burke oviDN SLP.FLA.8 720575940632512156 Austin T Burke, Varun Sane, Katharina Einer oviDN SLP.FLA.3 720575940640872923 Joseph Hsu, Greg Jefferis oviDN SMP.FLA.45 720575940621257340 Varun Sane, A. Javier oviDNa SMP.FLA.13 720575940613316783 Yijie Yin, Arti Yadav, Márcia Santos, Zhiha	Interneuron	SLP.SMP.32	720575940637878854	Burke
Interneuron AVLP.SLP.9 720575940604516524 Jay Gager, Nash Hadjerol, Dharini Sapka Interneuron SLP.SMP.67 720575940604395436 Jay Gager, Austin T Burke Interneuron SLP.457 720575940626446850 Austin T Burke, Varun Sane, J. Anthony C Dhara Kakadiya Interneuron SLP.52 720575940624247787 Varun Sane, Chitra Nair, Yijie Yin, Yashvi Interneuron SLP.378 720575940621569635 Austin T Burke oviDN SLP.FLA.8 720575940632512156 Austin T Burke, Varun Sane, Katharina Einer oviDN SLP.FLA.3 720575940640872923 Joseph Hsu, Greg Jefferis oviDN SMP.FLA.45 720575940621257340 Varun Sane, A. Javier oviDNa SMP.FLA.13 720575940613316783 Yijie Yin, Arti Yadav, Márcia Santos, Zhiha	Interneuron	AVLP.SLP.36	720575940617406548	1 -
Interneuron SLP.SMP.67 720575940604395436 Jay Gager, Austin T Burke Interneuron SLP.457 720575940626446850 Austin T Burke, Varun Sane, J. Anthony C Dhara Kakadiya Interneuron SLP.52 720575940624247787 Varun Sane, Chitra Nair, Yijie Yin, Yashvi Interneuron SLP.378 720575940621569635 Austin T Burke oviDN SLP.FLA.8 720575940632512156 Austin T Burke, Varun Sane, Katharina Eine oviDN SLP.FLA.3 720575940640872923 Joseph Hsu, Greg Jefferis oviDN SMP.FLA.45 720575940621257340 Varun Sane, A. Javier oviDNa SMP.FLA.13 720575940613316783 Yijie Yin, Arti Yadav, Márcia Santos, Zhiha	Interneuron	AVLP.SLP.42	720575940628351217	Nash Hadjerol, Austin T Burke, Joshua Bañez
Interneuron SLP.457 720575940626446850 Austin T Burke, Varun Sane, J. Anthony C Dhara Kakadiya Interneuron SLP.52 720575940624247787 Varun Sane, Chitra Nair, Yijie Yin, Yashvi Interneuron SLP.378 720575940621569635 Austin T Burke oviDN SLP.FLA.8 720575940632512156 Austin T Burke, Varun Sane, Katharina Ei oviDN SLP.FLA.3 720575940640872923 Joseph Hsu, Greg Jefferis oviDN SMP.FLA.45 720575940621257340 Varun Sane, A. Javier oviDNa SMP.FLA.13 720575940613316783 Yijie Yin, Arti Yadav, Márcia Santos, Zhiha	Interneuron	AVLP.SLP.9	720575940604516524	Jay Gager, Nash Hadjerol, Dharini Sapkal
Dhara Kakadiya	Interneuron	SLP.SMP.67	720575940604395436	
Interneuron SLP.378 720575940621569635 Austin T Burke oviDN SLP.FLA.8 720575940632512156 Austin T Burke, Varun Sane, Katharina Eigen Varun Sane, Katharina Eigen Surger oviDN SLP.FLA.3 720575940640872923 Joseph Hsu, Greg Jefferis oviDN SMP.FLA.45 720575940621257340 Varun Sane, A. Javier oviDNa SMP.FLA.13 720575940613316783 Yijie Yin, Arti Yadav, Márcia Santos, Zhiha	Interneuron	<u>SLP.457</u>	720575940626446850	
oviDN SLP.FLA.8 720575940632512156 Austin T Burke, Varun Sane, Katharina Ei oviDN SLP.FLA.3 720575940640872923 Joseph Hsu, Greg Jefferis oviDN SMP.FLA.45 720575940621257340 Varun Sane, A. Javier oviDNa SMP.FLA.13 720575940613316783 Yijie Yin, Arti Yadav, Márcia Santos, Zhiha	Interneuron	<u>SLP.52</u>	720575940624247787	Varun Sane, Chitra Nair, Yijie Yin, Yashvi Patel
oviDN SLP.FLA.3 720575940640872923 Joseph Hsu, Greg Jefferis oviDN SMP.FLA.45 720575940621257340 Varun Sane, A. Javier oviDNa SMP.FLA.13 720575940613316783 Yijie Yin, Arti Yadav, Márcia Santos, Zhiha	Interneuron	<u>SLP.378</u>	720575940621569635	Austin T Burke
oviDN SMP.FLA.45 720575940621257340 Varun Sane, A. Javier oviDNa SMP.FLA.13 720575940613316783 Yijie Yin, Arti Yadav, Márcia Santos, Zhiha	oviDN	SLP.FLA.8	720575940632512156	Austin T Burke, Varun Sane, Katharina Eichler
oviDNa SMP.FLA.13 720575940613316783 Yijie Yin, Arti Yadav, Márcia Santos, Zhiha	oviDN	SLP.FLA.3	720575940640872923	Joseph Hsu, Greg Jefferis
	oviDN	SMP.FLA.45	720575940621257340	
	oviDNa	SMP.FLA.13	720575940613316783	Yijie Yin, Arti Yadav, Márcia Santos, Zhihao Zheng, A. Javier
oviDNa SMP.VES.13 720575940642312136 Austin T Burke, Varun Sane	oviDNa	SMP.VES.13	720575940642312136	Austin T Burke, Varun Sane

Table S3. Proofreading credits for connectome neurons, Related to STAR Methods
Details of the connectome neurons used in this study and those credited with more than 10% of the proofreading edits for the reconstructed cells.